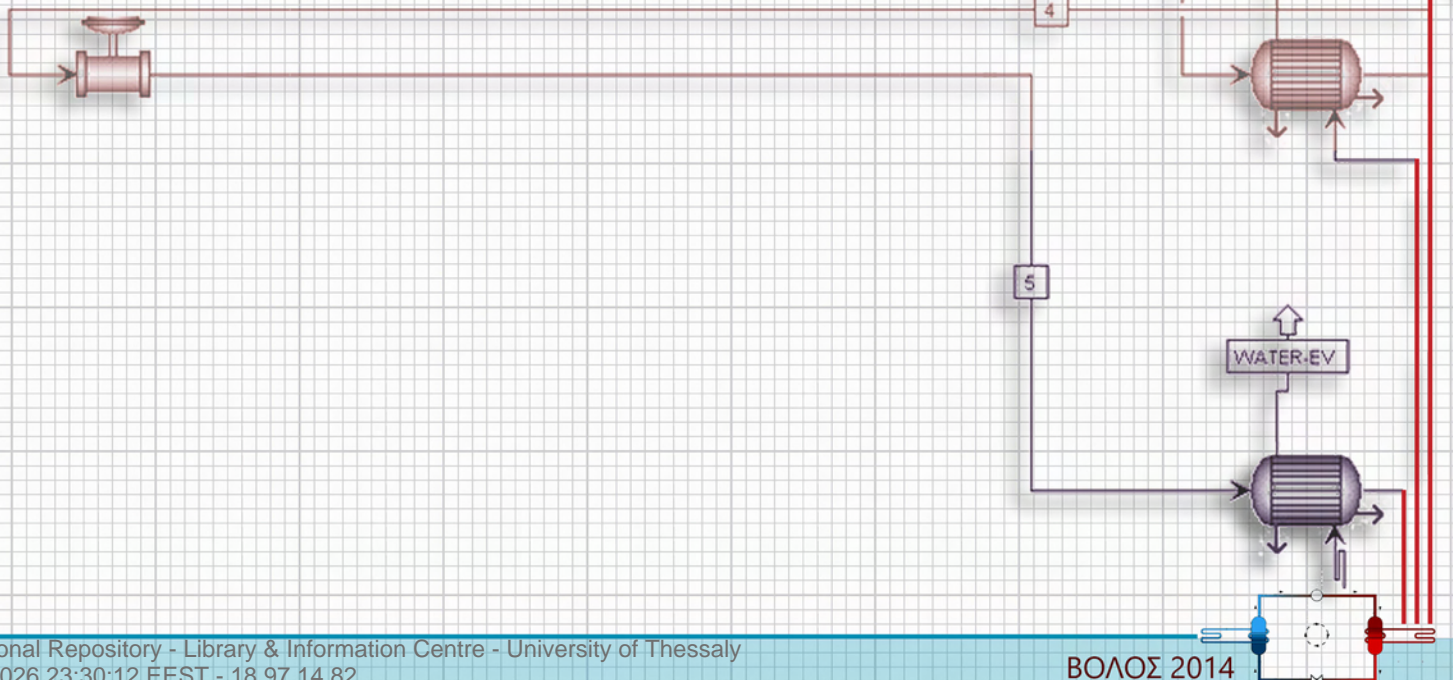




**ΜΕΤΑΠΤΥΧΙΑΚΗ ΕΡΓΑΣΙΑ**

**ΘΕΜΑ: Design and optimization of heat pump  
with transcritical cycle of CO<sub>2</sub>**

**ΦΟΙΤΗΤΗΣ: ΑΠΟΣΤΟΛΟΣ ΓΚΟΥΝΤΑΣ**  
**ΕΠΙΒΛΕΠΩΝ: ΑΝΑΣΤΑΣΙΟΣ ΣΤΑΜΑΤΗΣ**



© 2014 [Απόστολος Γκούντας](#)

Η έγκριση της μεταπτυχιακής εργασίας από το Τμήμα Μηχανολόγων Μηχανικών της Πολυτεχνικής Σχολής του Πανεπιστημίου Θεσσαλίας δεν υποδηλώνει αποδοχή των απόψεων του συγγραφέα (Ν. 5343/32 αρ. 202 παρ. 2).



## ***Advisor committee***

Advisor: Dr. Stamatis Anastassios  
Associate Professor, Department of Mechanical Engineering,  
University of Thessaly

Second member: Dr. Andritsos Nikolaos  
Professor, Department of Mechanical Engineering,  
University of Thessaly

Third member: Dr. Bontozoglou Vasilis  
Professor, Department of Mechanical Engineering,  
University of Thessaly

## ***Acknowledgements***

First of all, I would like to thank from the deep of my heart, my advisor Dr. Tassos Stamatis for the cooperation and his confidence from my undergraduate years. He had been always the inspiration to continue studying during this very difficult period of accomplishing my master thesis and his contribution to the conformation of my way of thinking and working was determinant.

Furthermore, I want to express my great thanks to all the professors that contributed to complete my Master and acquire all this scientific knowledge.

Finally, I would like to thank so much my family that was beside me during all this period, by supporting and encouraging me.

## Abstract

A CO<sub>2</sub> heat pump system was one of the first systems that were developed, but it was not widely used because of its low critical point and because there were other refrigerants that presented better performance in wider range of conditions. However, there was a revival at the beginning of 1990's, due to environmental concerns over HCFC's, unlike carbon dioxide's environmental friendliness. During the accomplishment of this thesis, an analytical literature review in the subject of heat pumps using transcritical cycle of CO<sub>2</sub> was carried out. Subsequently, the components of the system were modeled thermodynamically and a simulation of the performance of various models was fulfilled, based on some of the modifications that are applied to improve such systems' performance, such as the use of an internal heat exchanger and the use of capillary tubes for the expansion instead of throttling valve. Furthermore, after design and simulation of these heat pumps, optimization took place concerning COP, heating and cooling capacity using EES (Engineering Equation Solver) software. Finally, a comparative analysis took place, which refers to the results of simulation and optimization among the cycle modifications of the system's components.

# Contents

Advisor committee.....	3
Acknowledgements.....	4
Abstract.....	5
Contents.....	6
Figures.....	7
Nomenclature.....	9
1. Introduction.....	11
1.1. Main objectives of the thesis.....	11
1.2. Contents of the thesis.....	11
2. Transcritical CO <sub>2</sub> heat pumps operation.....	12
2.1. A brief historical review of the CO <sub>2</sub> 's use as a refrigerant.....	12
2.2. Revival of CO <sub>2</sub> as refrigerant.....	13
2.3. Conventional and transcritical heat pumps.....	15
2.4. Optimization of transcritical cycle of CO <sub>2</sub> .....	18
2.5. Cycle modifications.....	20
2.5.1. Internal heat exchanger.....	20
2.5.2. Compression modifications.....	22
2.5.3. Expansion modifications.....	25
3. Modeling of transcritical CO <sub>2</sub> heat pump systems.....	30
3.1. Thermodynamic analysis.....	31
3.1.1. Gas Cooler.....	32
3.1.2. Evaporator.....	33
3.1.3. Compressor.....	35
3.1.4. Expansion device.....	37
3.1.5. Internal heat exchanger.....	38
3.2. Transport characteristics of CO <sub>2</sub> .....	38
3.2.1. Supercritical cooling (Gas-cooler Analysis).....	39
3.2.2. Flow boiling (Evaporator Analysis).....	42
3.3. Modeling software tool EES (Engineering Equation Solver).....	44
4. Results and discussion.....	48
4.1. Input parameters and calculation flowchart.....	48

4.2. Basic TCHP model.....	50
4.3. TCHP model with internal heat exchanger (IHEX) .....	54
4.4. TCHP model with expansion recovery work with turbine .....	58
5. Conclusions .....	63
6. Future work.....	64
Bibliography .....	65

## Figures

Figure 1. P-T phase diagram for CO <sub>2</sub> .....	14
Figure 2. Transcritical cycle of CO <sub>2</sub> and heat pump arrangement.....	15
Figure 3. Heat pump cycle with condenser (conventional) or gas cooler (transcritical).....	16
Figure 4. A photo of a heat exchanger that is used as gas cooler .....	17
Figure 5. P-h diagram for (a) subcritical and (b) transcritical cycle .....	17
Figure 6. Schematic diagram of TCHP with internal heat exchanger .....	21
Figure 7. T-S diagram of TCHP with internal heat exchanger .....	21
Figure 8. TCHP with 2-stage compression and intercooling.....	22
Figure 9. TCHP with flash intercooling (a) schematic diagram (b) cycle diagram P-h .....	23
Figure 10. Schematic and corresponding P–h diagrams for two-stage cycle with flash gas bypass .....	23
Figure 11. Layout and p-h diagram of refrigeration cycle with parallel compression economization .....	24
Figure 12. Schematic diagram of an auxiliary loop TCHP system.....	25
Figure 13. Section of a non-adiabatic capillary tube heat exchanger [11].....	26
Figure 14. P-h diagram of TCHP with expansion through capillary tube.....	26
Figure 15. Schematic diagram and P-h diagram of transcritical CO <sub>2</sub> system with expansion turbine [6] .....	28
Figure 16. Transcritical CO <sub>2</sub> system with ejector expander: (a) Schematic diagram, (b) P-h diagram [1].....	29
Figure 17. A computational segment of heat exchangers.....	30
Figure 18. A photograph of ground source CO <sub>2</sub> air conditioning and heat pump system [18] ...	31
Figure 19. Discretization of a double-tube counter flow gas cooler .....	32
Figure 20. Evaporator .....	34
Figure 21. CO <sub>2</sub> compressor .....	35
Figure 22. Comparison of experimental data with the calculated heat transfer coefficients using existing correlations as a function of carbon dioxide temperature [20].....	39
Figure 23. Schematic diagram of stratified two-phase flow in a horizontal tube .....	44
Figure 24. Code and formatted equations from EES .....	45
Figure 25. Variable info windows, where we can set guess values and variable limits .....	46
Figure 26. Property plot derived from EES .....	46

Figure 27. Parametric table derived from EES.....	47
Figure 28. Flowchart for the transcritical CO <sub>2</sub> heat pump system .....	49
Figure 29. TCHP without IHEX designed with ASPEN .....	50
Figure 30. TCHP with IHEX designed with ASPEN .....	54
Figure 31. TCHP with an expansion turbine designed with ASPEN .....	58

## Tables

Table 1. Table presents GWP for CO <sub>2</sub> and other HFC's [3] .....	13
Table 2. Refrigerants' characteristics and properties [4] .....	14
Table 3. Table for friction factors correlations for pressure drop calculation .....	41
Table 4. Components specifications .....	48
Table 5. Input properties variables .....	48
Table 6. Table with properties values as model output .....	51
Table 7. Table with properties values as output from TCHP with IHEX model .....	55
Table 8. Properties values as output from TCHP model with turbine .....	59

## Graphs

Graph 1. Plot of isentropic compressor efficiency versus pressure ratio using equation (22) and correlation proposed by Robinson & Groll [7].....	37
Graph 2. T-s diagram of TCHP model.....	51
Graph 3. P-h diagram of TCHP model.....	52
Graph 4. COP vs discharge pressure .....	52
Graph 5. Heating capacity variation over discharge pressure.....	53
Graph 6. T-s diagram for TCHP with IHEX.....	55
Graph 7. P-h diagram for TCHP with IHEX .....	56
Graph 8. COP variation over compressor speed for TCHP with IHEX.....	57
Graph 9. COP variation respect to length of IHEX .....	57
Graph 10. T-s diagram with TCHP model with an expansion turbine .....	59
Graph 11. P-h diagram with TCHP model with an expansion turbine.....	60
Graph 12. COP variation over compressor's rotational speed .....	61
Graph 13. COP variation over discharge pressure for TCHP with an expansion turbine .....	62
Graph 14. Contour for COP as a function of discharge pressure and compressor's speed .....	62

# Nomenclature

COP	coefficient of performance
P	Pressure (bar)
T	absolute temperature (K or °C)
h	specific enthalpy (kJ/kg)
$h_{fg}$	latent heat of vaporization (J/kg)
$\dot{m}$	mass flow (kg/s)
R	gas constant (kJ kg <sup>-1</sup> K <sup>-1</sup> )
s	specific entropy (kJ kg <sup>-1</sup> K <sup>-1</sup> )
W	work (W)
Q	heat energy (W)
UA	overall heat transfer coefficient area of transfer product (W/K)
A	heat transfer area (m <sup>2</sup> )
$c_p$	specific heat (kJ kg <sup>-1</sup> K <sup>-1</sup> )
Nu	Nusselt number
Pr	Prandtl number
Re	Reynolds number
k	thermal conductivity (W m <sup>-1</sup> K <sup>-1</sup> )
$k_w$	wall thermal conductivity (W m <sup>-1</sup> K <sup>-1</sup> )
N	compressor speed (rpm)
$V_s$	swept volume of compressor (m <sup>3</sup> )
$h_r$	heat transfer coefficient (W m <sup>-1</sup> K <sup>-1</sup> )
$d_i$	inner diameter (m)
$d_o$	outer diameter (m)
f	friction factor
$\rho$	density (kg/ m <sup>3</sup> )
x	quality
Bo	boiling number
Bd	Bond number
M	molecular weight
$\vartheta$	angle (deg)
$X_{tt}$	Martinelli's factor

## Greek symbols

$\varepsilon$	effectiveness
$\eta_{is}$	Isentropic efficiency

## Subscripts

1-4	refrigerant state points
5-8	external fluid state points
s	isentropic process
ev	evaporator

gc	gas cooler
comp	compressor
opt	optimum
i	input
o	output
w	water
r	refrigerant
rb	refrigerant bulk
rw	refrigerant wall
cr	critical
nb	nucleate boiling
l	liquid
g	gas
tp	two-phase
suc	suction
dis	discharge

# 1. Introduction

## 1.1. Main objectives of the thesis

Carbon dioxide is a safe, economic and environmentally sustainable refrigerant which can be used in heat pump and refrigeration systems. The study of the heat pumps, which use transcritical cycle of carbon dioxide, and consist a modern and innovative object that is being studied by researchers all over the world, was the main objective of this thesis. Main goal of our project was the bibliographic review over transcritical cycle of CO<sub>2</sub> heat pumps (TCHP) and the thermodynamic modeling and simulation of such systems.

An additional objective of the thesis was the familiarity with software tools, such as EES that can simulate any thermodynamic problem. The work presented here concern the development of some models, using EES, which can predict the performance of a TCHP system, including some of the modifications that can be applied in such systems.

## 1.2. Contents of the thesis

The thesis is consisted by 4 chapters. Chapter 2 includes a historical review of CO<sub>2</sub> as refrigerant and heat pumps' cycle, including the possible modifications. Chapter 3 includes the modeling of the transcritical cycle of heat pumps with carbon dioxide and the thermodynamic equations governing the operation of different components of the system, presenting also the software tool EES that is used and finally, Chapter 4 includes the input parameters, the results and the discussion over the simulation and the optimization that is carried out.

## 2. Transcritical CO<sub>2</sub> heat pumps operation

### 2.1. A brief historical review of the CO<sub>2</sub>'s use as a refrigerant

A carbon dioxide based heat pump system was one of the first systems that were developed, but it was not widely used because of its low critical point and because there were other refrigerants that presented better performance in wider range of conditions. However, after Montreal protocol that abolished the use of CFC and HCFC as refrigerants, because of their harmful environmental behavior, began a growing research into the performance and benefits of a transcritical heat pump cycle using carbon dioxide. Using the natural working fluids as refrigerants was advocated by Lorentzen at the beginning of 1990's. Among these natural refrigerants, the carbon dioxide (CO<sub>2</sub>) has gained much more attention owing to its no toxicity, no flammability, low cost and no hazard to the environment, excellent transport properties, compatibility with various common material, etc.

Heat pump systems are closely related to refrigeration systems, but vapor compression cycles were developed for refrigeration long before the concept was applied to heating. Likewise, refrigerant fluids were developed for refrigeration rather than heating. Carbon dioxide was among the first refrigerants used in commercially viable vapor compression refrigeration systems. Other early refrigerants included ether, ammonia, sulfur dioxide and methyl chloride. CO<sub>2</sub> was first used in a vapor compression system to produce ice. The high working pressures of CO<sub>2</sub> were a hindrance to implementation, allowing ammonia and sulfur dioxide systems to become established first.

Ammonia systems were generally efficient, but they were quite large and ammonia's toxic nature presented a safety hazard. In comparison, CO<sub>2</sub> required more fuel and more robust components, but the systems were much smaller and CO<sub>2</sub> leaks did not pose a health risk.

For its improved safety and compactness ships began to use CO<sub>2</sub> for refrigeration in the 1880s and 90s, while on land ammonia was dominant. A further reason for the divergence of land and sea systems respectively to ammonia and CO<sub>2</sub> was condensing temperature and means of condensing. Due to CO<sub>2</sub>'s low critical temperature, significant loss of capacity and efficiency occur as condenser temperature increases. Ammonia can operate under a wider range of condenser temperatures. Early systems mainly used river or sea water as the heat sink for condensing. This provided the low temperatures required for CO<sub>2</sub>. Later, evaporative coolers were utilized when a body of water was unavailable. Evaporative coolers generally produce higher condensing temperatures which favored ammonia over CO<sub>2</sub> [1].

## 2.2. Revival of CO<sub>2</sub> as refrigerant

Interest in CO<sub>2</sub> was renewed in the early 1990's in part due to the phase-out of ozone depleting refrigerants. Norwegian professor Gustav Lorentzen has received much of the credit for the new attention given to CO<sub>2</sub>, as he studied many applications using transcritical cycle of CO<sub>2</sub>. By then research into CO<sub>2</sub> refrigeration, air-conditioning and heat pump systems continues, but some CO<sub>2</sub> systems have already been successfully commercialized.

Climate change is a major worldwide concern with potentially dramatic impacts on developing and industrialized countries alike. The effort to mitigate climate change centers on the reduction of greenhouse gas emissions. The global warming potential (GWP) is a relative measure of the heat trapping effect of a gas in comparison to an equal mass of carbon dioxide over a given quantity of time in the atmosphere. HFC's have a global warming potential that is enormous relatively to CO<sub>2</sub>. Typically, a kilogram of HFC contributes 1000-3000 times more to the global warming, than release from a kilogram of CO<sub>2</sub> [2]. This is the reason why these gases are included in the Kyoto-agreement as compounds to be regulated.

Refrigerant	CFC12	HCFC22	HFC134a	NH <sub>3</sub> R717	C <sub>3</sub> H <sub>8</sub> R290	CO <sub>2</sub>
Natural substance	No	No	No	Yes	Yes	Yes
ODP	1.0	0.05 <sup>a</sup>	0	0	0	0
GWP <sup>b</sup>						
100 years	7100	1500	1200	0	0	1(0) <sup>c</sup>
20 years	7100	4100	3100			1(0)
TLV <sub>8h</sub> (ppm)	1000	1000	1000 <sup>d</sup>	25	1000	5000
IDLH <sup>e</sup>	50000	-	-	500	20000	50000
Amount per room vol <sup>f</sup> (vol%/kg m <sup>-3</sup> )	4.0/0.2	4.2/0.15	-	-	0.44/0.008	5.5/0.1
Flammable or explosive?	No	No <sup>a</sup>	No <sup>a</sup>	Yes	Yes	No
Flammability limits in air (vol%)	-	-	-	15.5/27	2.2/9.5	-
Toxic/irritating decomposition products?	Yes	Yes	Yes	No	No	No
Approx. relative price	1	1	3-5	0.2	0.1	0.1
Molar mass	120.92	86.48	102.03	17.03	44.1	44.01
Volumic <sup>h</sup> refr. capacity at 0 °C (kJ m <sup>-3</sup> )	2740	4344	2860	4360	3870	22600

**Table 1.** Table presents GWP for CO<sub>2</sub> and other HFC's [3]

Two factors require special attention when using CO<sub>2</sub> as a refrigerant for heat pump systems. One is the low critical temperature, since CO<sub>2</sub> becomes supercritical fluid at 31.1 °C at 73.7 bar. The other is the high working pressure required to use CO<sub>2</sub> under typical heat pump conditions.

Working fluid	R-22	R-134a	R-290	R-600	R-600a	R-1270	R-717	R-744
Chemical formula	CHClF <sub>2</sub>	CF <sub>3</sub> CH <sub>2</sub> F	C <sub>3</sub> H <sub>8</sub>	C <sub>4</sub> H <sub>10</sub>	C <sub>4</sub> H <sub>10</sub>	C <sub>3</sub> H <sub>6</sub>	NH <sub>3</sub>	CO <sub>2</sub>
Molar mass (g mol <sup>-1</sup> )	86.46	102.03	44.10	58.12	58.12	42.08	17.03	44.01
Critical temperature (°C)	96.14	101.0	96.7	152.0	134.7	92.4	131.9	31.1
Critical pressure (kPa)	4990	4067	4247	3796	3640	4665	11333	7384
Critical density (kg m <sup>-3</sup> )	562.0	552.5	220.0	227.8	224.4	222.6	225.0	466.5
Boiling point <sup>a</sup> (°C)	-40.9	-26.1	-42.1	-0.5	-11.6	-47.7	-33.3	-78.4
Flammability	No	No	Yes	Yes	Yes	Yes	Yes	No
Toxicity	No	No	No	No	No	No	Yes	No
ODP	0.05	0	0	0	0	0	0	0
GWP <sup>c</sup>	1700	1300	3	3	3	3	0	1

<sup>a</sup> Boiling point at atmospheric pressure

<sup>b</sup> At 20 °C

<sup>c</sup> Reference to CO<sub>2</sub> with base values of 1

**Table 2.** Refrigerants' characteristics and properties [4]

In a conventional (subcritical) heat pump cycle, low critical temperature ( $T_{crit}$ ) is a disadvantage because it limits the operating temperature range, as heat cannot be delivered at temperatures greater than the critical temperature. Furthermore, at temperatures less than but near  $T_{crit}$ , the enthalpy of vaporization is reduced. This leads to a reduction in heating capacity and poor performance of the system[3]. However, CO<sub>2</sub>'s low critical temperature provides the opportunity to operate in a transcritical manner.

High working pressure is the other notable distinction of CO<sub>2</sub> heat pumps. Both subcritical and transcritical heat pump systems using CO<sub>2</sub> operate at pressures greater than with most other refrigerants. Subcritical CO<sub>2</sub> heat pumps may function at pressures as high as 60–70 bar, while transcritical systems may have pressures from 80 to 110 bar or more. For comparison, R134a has a saturation pressure of 13.18 bar at 50 °C [1].

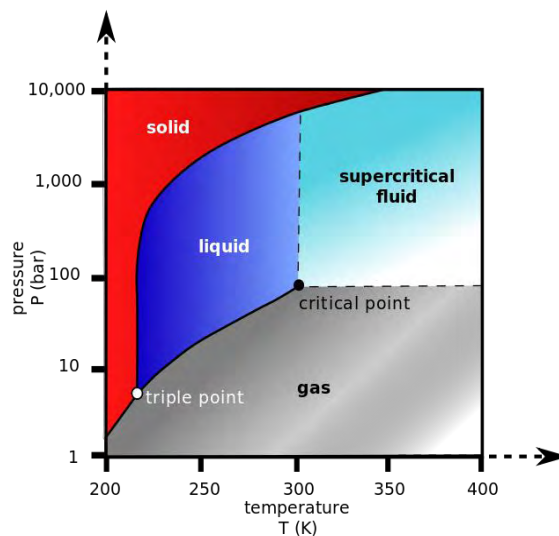


**Figure 1.** P-T phase diagram for

When CO<sub>2</sub> started losing market shares around 1940, the lack of components that can operate at such conditions was one of the reasons for the decline. However, with the manufacturing technology and the knowledge base existing today, it is possible to manufacture such components and take advantage of the benefits of a transcritical cycle of carbon dioxide.

A transcritical cycle of carbon dioxide and a typical heat pump that operates this cycle are presented in the Figure 2.

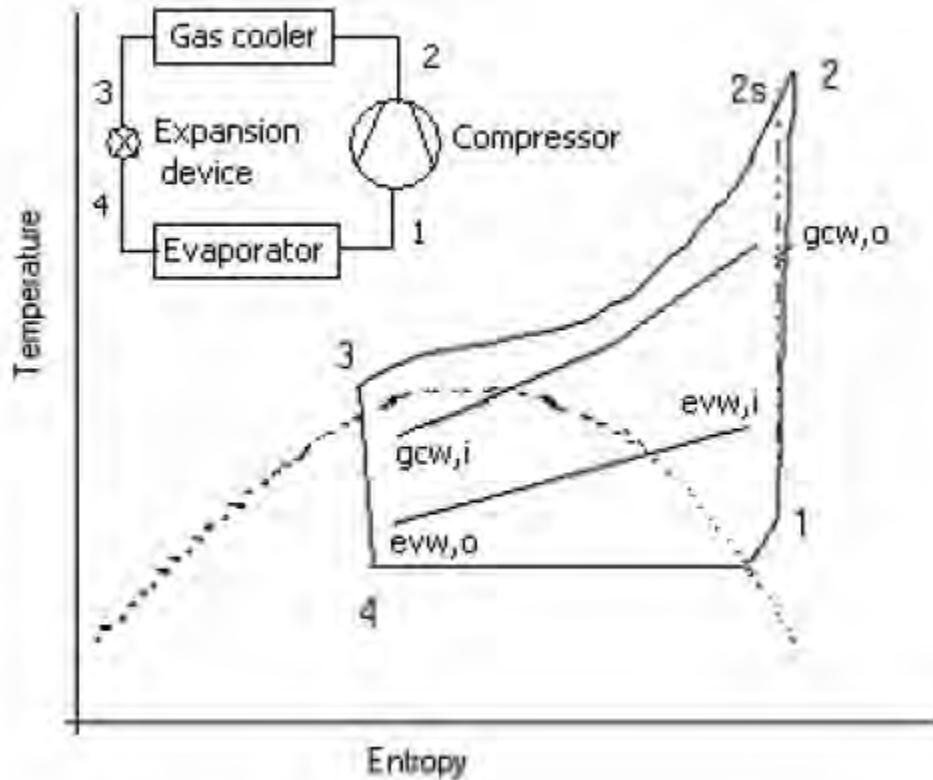


**Figure 2.** Transcritical cycle of CO<sub>2</sub> and heat pump arrangement

### **2.3. Conventional and transcritical heat pumps**

A heat pump is a device that provides heat energy from a source of heat that has lower temperature to a warmer destination that is called heat sink. Opposite to internal combustion engines and electrical resistances, heat pumps are not designed to produce thermal energy. A heat pump uses some amount of external power to accomplish the work of transferring energy

from the heat source to the heat sink. Heat pumps are used mainly for usual freezers or air conditioners, but also apply to many heating, ventilation and air conditioning (HVAC) systems.

In the conventional heat pumps, the entire cycle takes place below the critical point of the refrigerant, which is in use. Heat absorption occurs by evaporation of the refrigerant at low pressure, and heat rejection takes place by condensing the high pressure refrigerant.

In heat pump that uses a transcritical cycle, an evaporator still serves the heat absorption function, but heat rejection is not through condensation. The refrigerant pressure is increased into the supercritical region, and heat rejection occurs by single-phase sensible cooling (gas cooling), so in a transcritical cycle heat rejection takes place via a gas cooler rather than a condenser.

A typical heat pump system that operates transcritical cycle of carbon dioxide includes the following components (Figure 3):

- Compressor – increases CO<sub>2</sub>'s pressure and temperature
- Gas cooler – heat-exchanger for CO<sub>2</sub> cooling (Figure 4)
- Expansion valve – expands the fluid and converts it to a two-phase fluid
- Evaporator – heat-exchanger that evaporates fully the fluid by heat absorption

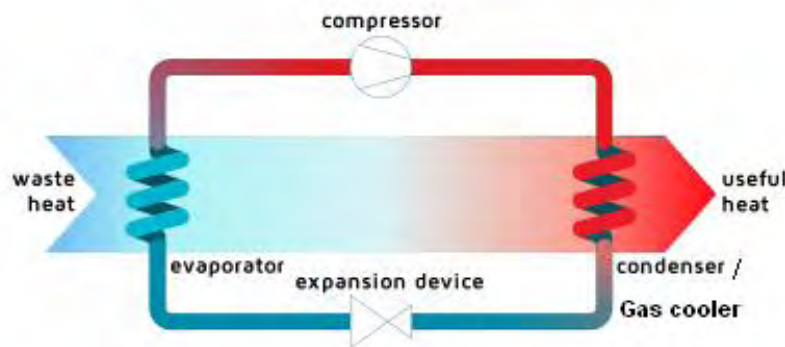


**Figure 3.** Heat pump cycle with condenser (conventional) or gas cooler (transcritical)

Anything different or further to these components is not included in the basic transcritical CO<sub>2</sub> heat pump (TCHP) cycle, but consists a part of the modifications that can improve the system and will be analyzed later.



**Figure 4.** A photo of a heat exchanger that is used as gas cooler

The cycle that was proposed from Lorentzen [4] for transcritical cycle of carbon dioxide and is the common cycle that is used in the majority of scientific studies is presented in Figure 5 b and operates with the following cycle:

1. 1→2: Isentropic compression
2. 2→3: Isobaric cooling
3. 3→4: Isentropic expansion
4. 4→1: Isobaric heating

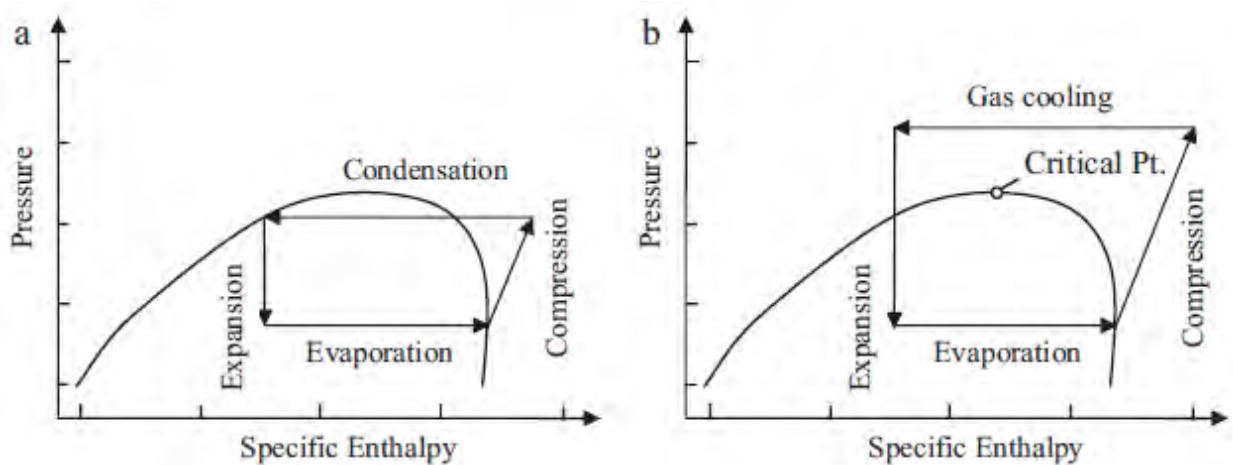


**Figure 5.** P-h diagram for (a) subcritical and (b) transcritical cycle

The efficiency of this cycle, according to Lorentzen, is given by the following relationship:

$$COP = \frac{Q}{W} = \frac{T_{2s} - T_3}{(T_{2s} - T_3) - T_0 \cdot \ln\left(\frac{T_{2s}}{T_3}\right)} \quad (1)$$

To make effective use of the transcritical cycle, the large pressure difference and the uniqueness of the gas cooling process must be addressed. Optimization of the transcritical cycle depends on the components and various operating parameters which are different from the conventional cycle. Certain heating applications benefit from the unique characteristics of the transcritical cycle. An example is heating applications that require a very large temperature increase. Since the gas cooler rejects heat by sensible cooling, the difference between the inlet and outlet temperatures (temperature glide) is much greater than in a condensing process. Thus the transcritical cycle is more beneficial for heating applications requiring large temperature increase.

The pressure difference between the heat rejection pressure (gas cooler pressure) and the heat absorption pressure (evaporator pressure) is much greater in a transcritical CO<sub>2</sub> system than in a typical subcritical system. This results in large thermodynamic losses during the expansion process. However, the large pressure difference also makes it feasible to implement an expansion work recovery device into the system. Expansion work recover could partially compensate the throttling losses of transcritical CO<sub>2</sub> heat pumps.

## **2.4. Optimization of transcritical cycle of CO<sub>2</sub>**

There are many factors that determine the performance for a single-stage CO<sub>2</sub> heat pump and we can vary them in order to optimize the Coefficient of Performance (COP) of our system. The main factors that do this are:

- Evaporator – the evaporation temperature ( $T_{ev}$ )
- Compressor – the overall isentropic efficiency ( $\eta_{is}$ )
- Gas cooler – the mean temperature during heat rejection ( $T_m$ )
  - The optimum gas cooler pressure ( $P_{gc}$ )
  - The CO<sub>2</sub> gas cooler outlet temperature ( $T_{gc}$ )
- Possible recovery if expansion energy
  - Ejector
  - Expander

Studies have concluded that there are optimum operating conditions corresponding to optimum COP and the knowledge of these optimum conditions is a very important factor in the design of a transcritical carbon dioxide cycle. The optimum discharge pressure is the most frequent optimized variable after COP's optimization, as the optimum pressure yields an optimum COP.

In the transcritical refrigeration cycle, the vapor from evaporator is compressed to supercritical (gas cooler) pressure, rejected heat at gliding temperature and expanded from supercritical pressure to subcritical (evaporator) pressure to give cooling. For the conventional cycle, condensing temperature is chosen based on coolant temperature in the condenser and corresponding saturated pressure is taken as the condensing pressure. But for supercritical heat rejection no saturation point exists, so the gas cooler pressure is independent of the refrigerant temperature at gas cooler exit (point 3 in Figure 2). In these systems, if gas cooler exit temperature is fixed, with appropriate inlet temperature of the external fluid and gas cooler design, as the pressure increases the COP increases initially and then the added capacity no longer compensates for the additional work of compression and hence COP decreases. So, there is an optimum discharge pressure that gives an optimum COP. The optimum discharge pressure and corresponding performance are dependent on evaporator temperature, gas cooler exit temperature, degree of superheat and compressor design. The optimum discharge pressure increases with increase in gas cooler exit temperature and decrease in evaporator temperature. There are many theoretical studies that deal with discharge pressure optimization and various proposed correlations have come off. The best proposed correlation based on experimental results is:

$$P_{d,opt} = 4.9 + 2.256 \cdot T_{gc} - 0.17 \cdot T_{ev} + 0.002 \cdot T_{gc}^2 \quad (2)$$

Furthermore, the carbon dioxide transcritical cycle can be optimized to the second (exergetic) thermodynamic law. In reality, the refrigeration cycle includes various irreversible processes. Exergy or availability of a system at given state represents its maximum work potential. Therefore, the exergy loss provides a very important criterion to evaluate the thermodynamic performance of a system. By analyzing the irreversibility of the system, it can be known how the actual cycle departs from the ideal cycle. Also, the optimization of the heat exchanger tube diameter and length and effect of design parameters on overall system performance can be obtained [5]. For effective sizing of heat exchangers, detailed knowledge of irreversibility is essential. For example, for the same capacity (constant mass flow rate), heat exchanger area can be reduced by reducing diameter, so that irreversibility due to material reduces; however, the irreversibility due to pressure drop will increase rapidly. To accommodate this, a multi-pass arrangement can be introduced using very small tubes (for example, in a microchannel heat exchanger), but this will give rise to higher manufacturing irreversibility. So it is not an easy task to choose an effective set of diameter, length and

number of passes for heat exchangers and hence the necessity of an optimization exercise arises [6].

## **2.5. Cycle modifications**

As it has been referred earlier, there are many factors that can determine the performance of a transcritical cycle of CO<sub>2</sub>. The improvement of overall cycle performance in a TCHP generally requires consideration of the system as a whole. The interactions between the components do not always allow for isolated improvements to a single component. Still, each component or process in the cycle plays a role in dictating the overall performance of the system. The major disadvantage of CO<sub>2</sub> cycle is lower COP due to huge expansion loss compared to conventional refrigerants and hence the cycle needs modifications. There are several reasons for modifying the basic single-stage transcritical cycle, including improvement of COP, the optimum discharge pressure, capacity enhancement for a given system and component size, adaptation of the heat rejection temperature profile to given requirements and keeping the pressure ratio and discharge temperature of the compressor within limit. In principle, a large number of possible modifications are possible, including staging of compression and expansion, splitting of flows, and work-generating expansion instead of throttling and huge researches have been carried out on several cycle modifications such as use of internal heat exchanger, expansion turbine, multi-staging, two-phase ejector, vortex tube, capillary tubes and parallel compression economization [6].

### **2.5.1. Internal heat exchanger**

A common addition to the most basic system is the internal heat exchanger (IHEx). An IHEx brings the discharge vapor of the gas cooler into thermal exchange with the discharge vapor of the evaporator by means of a counter-flow heat exchanger, as shown in Figure 6. The purpose of including an internal heat exchanger in a refrigeration cycle is to ensure vaporization of the refrigerant prior to compression and to attempt to recover stream availability following heat rejection in order to reduce power input to the compressor. Also, an IHEx serves to subcool the gas cooler vapor before it goes through the expansion process [7]. Generally, the modification of the IHEx contributes an increase about 4-7% in COP, but increases gas cooler pressure about 20%.

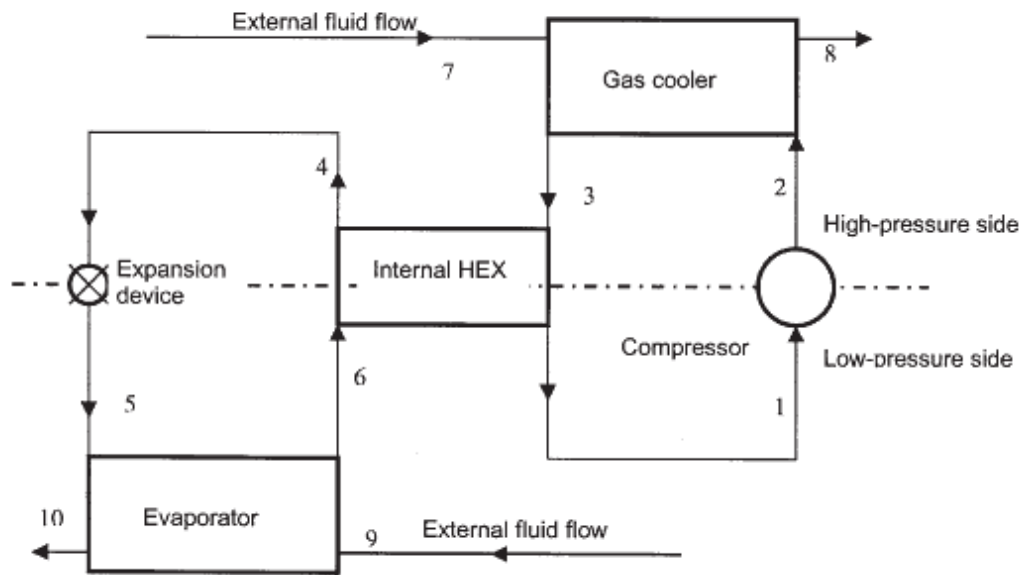


**Figure 6.** Schematic diagram of TCHP with internal heat exchanger

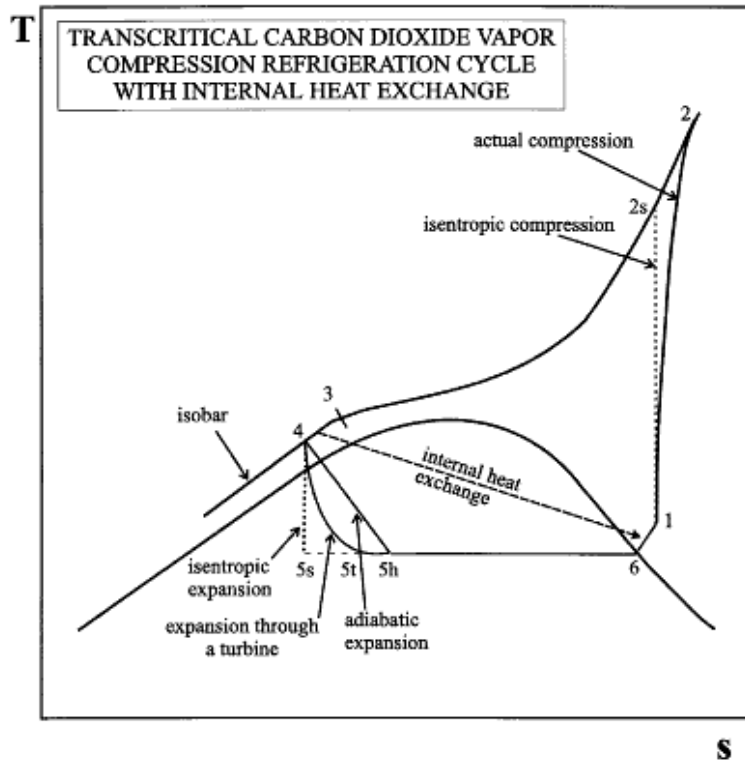


**Figure 7.** T-S diagram of TCHP with internal heat exchanger

## 2.5.2. Compression modifications

Efficiency of a TCHP can be improved by various modifications of the compression process. The most basic compressor modification is two-stage compression. By separating compression into two stages, each compressor will have a lower pressure ratio which in turn improves the isentropic efficiency. Further improvements in cycle efficiency can be obtained by cooling the refrigerant between the two stages.

Experimental study with two-stage compression with inter-cooling [8] confirmed that an optimum upper cycle pressure giving the maximum energy efficiency occurs for transcritical operation and up to 25% increase in the coefficient of performance was found for typical air conditioning applications. Simulation result shows that for evaporation temperature of  $-40\text{ }^{\circ}\text{C}$ , refrigerant temperature at gas cooler outlet of  $40\text{ }^{\circ}\text{C}$  and isentropic efficiencies of 70% for both compressors, the cooling COP (evaporative cooling output divided by work of both compressors) improves by about 12% and the optimum compressor discharge pressure reduces by 30% compared to single stage for a degree of inter-cooling of  $30\text{ }^{\circ}\text{C}$ . The results also showed that the benefits of inter stage cooling are strongly enhanced by the use of an internal heat exchanger.

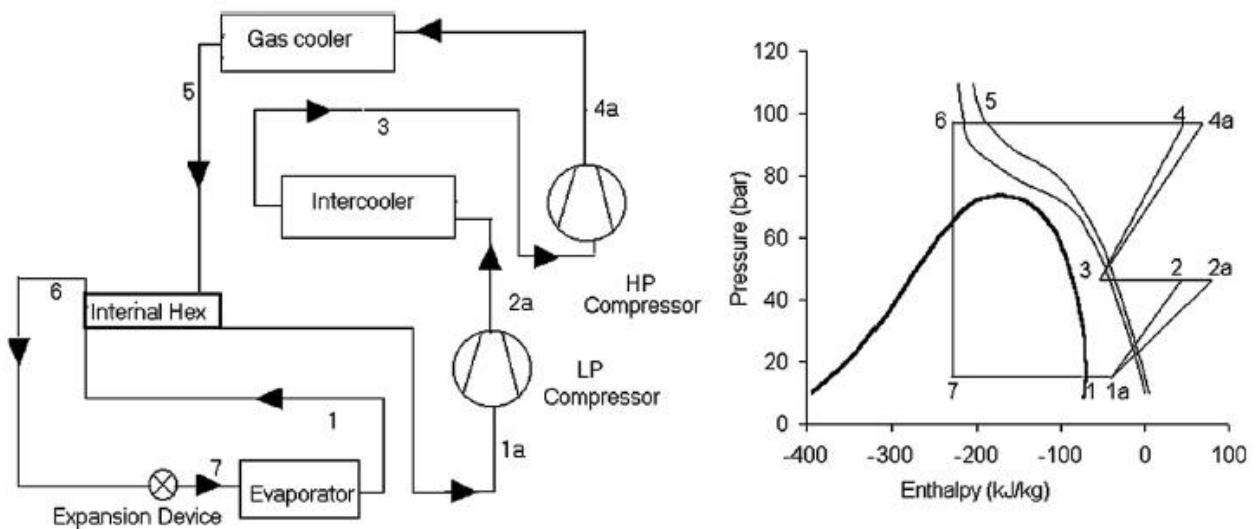
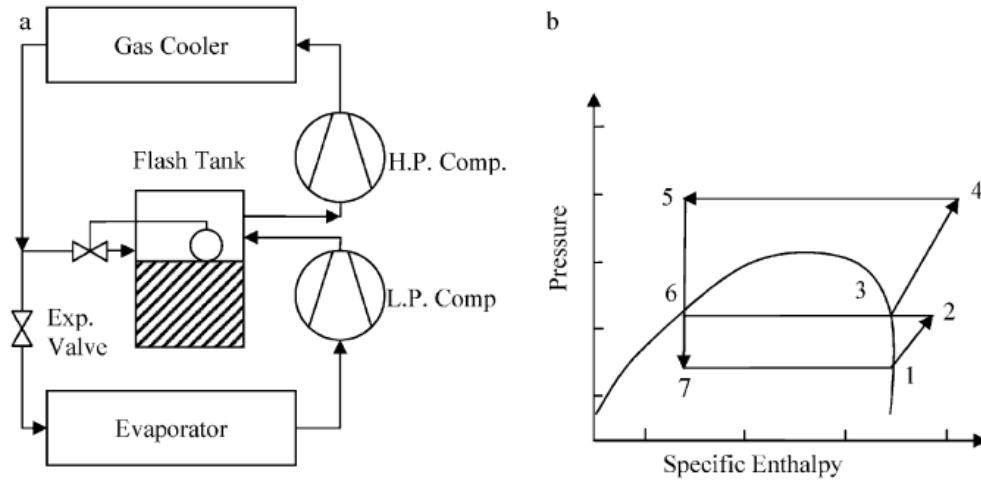


Figure 8. TCHP with 2-stage compression and intercooling

Beyond two stage compression with intercooling system, various systems can be configured which integrate modifications of both the expansion and compression processes. Flash intercooling is an alternative means of cooling the refrigerant between compression stages in which the inter-stage CO<sub>2</sub> temperature is reduced by mixing with expansion vapor in a flash tank (Figure 9). Studies have shown [9] that, unlike other methods of intercooling, two-stage compression with flash intercooling decreased the COP compared to that of an analogous system with single stage compression. This is due to the fact that mass flow rate through the

second stage compressor increases significantly. Though the specific work of compression in the second stage is reduced, actual compression work in the second stage increases. Intermediate pressure was found to have little impact on COP.



**Figure 9.** TCHP with flash intercooling (a) schematic diagram (b) cycle diagram P-h

Another two-stage CO<sub>2</sub> heat pump cycle is two-stage cycle with flash gas bypass. At Figure 10 we can see the two-stage CO<sub>2</sub> cycle with flash gas bypass (two-stage expansions through expansion valves and two-stage compressions are used with flash chamber). It is observed that the flash gas bypass system yields the best performance among the three two stage systems analyzed. Results also show that the deviation of optimum interstage pressure from the classical estimate, given by the geometric mean of the gas cooler and evaporator pressure increases as temperature lift increases.

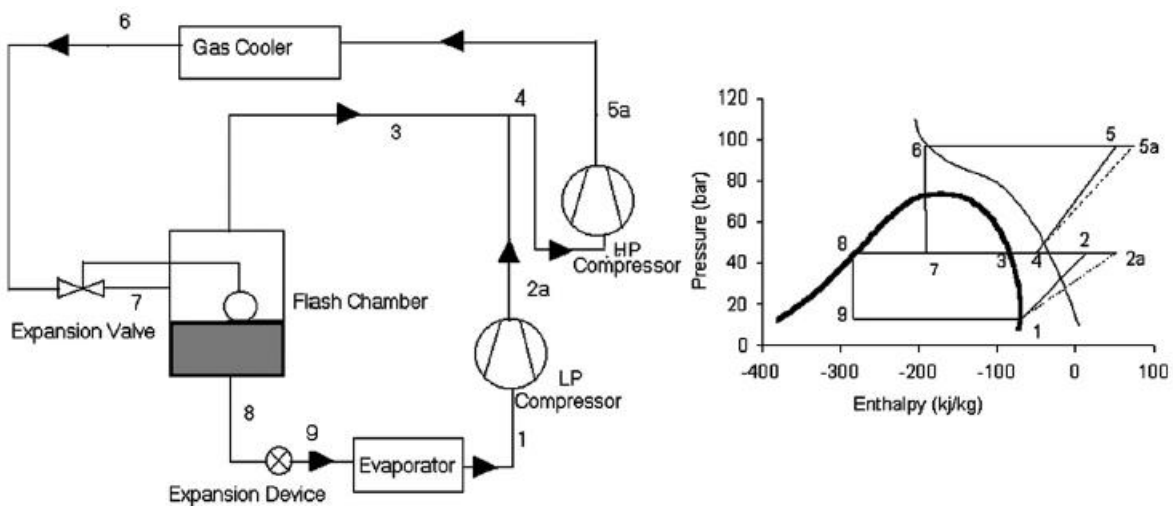


**Figure 10.** Schematic and corresponding P-h diagrams for two-stage cycle with flash gas bypass

More, the performance of transcritical CO<sub>2</sub> refrigeration cycle can be also improved by several percentages through the successful use of parallel compression economization. In parallel compression refrigerating system (Figure 11), after the expansion of transcritical fluid from states through primary expansion valve, the liquid (state 5) and vapour (state 7) are separated in economizer. The liquid is again expanded through another expansion valve and it extracts heat to give useful cooling effect in the evaporator (from states 6 to 1). In the compressor, refrigerant vapor is compressed to supercritical discharge pressure in two distinct non-mixing streams, one coming from the economizer and the other coming from the main evaporator. Subsequently, both the supercritical fluids mix and enter to the gas cooler for heat rejection to the external fluid. By parallel compression, quality of refrigerant decreases in evaporator and both refrigeration effect and compressor work increase, but increase in refrigeration effect is more than increase in compressor work, hence COP increases. Employing parallel compression economization is not only improves the optimum cooling COP but also brings down the optimum discharge pressure [6].

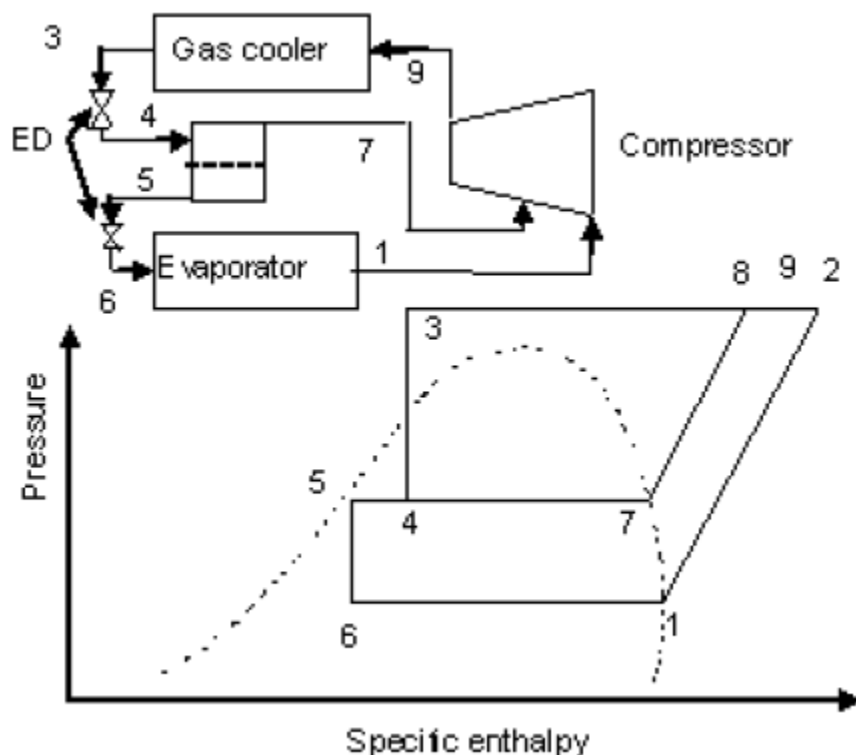


**Figure 11.** Layout and p-h diagram of refrigeration cycle with parallel compression economization

Finally, a transcritical system that has been analyzed, was composed of two different heat pump loops with independent compressors [10]. An internal heat exchanger served as the evaporator in the auxiliary loop while also subcooling the main-loop refrigerant prior to

expansion, as shown in Figure 12. Compared to heat pumps with more complicated dual compression cycles, the auxiliary cycle's cooling performance was better only for low intermediate pressures.

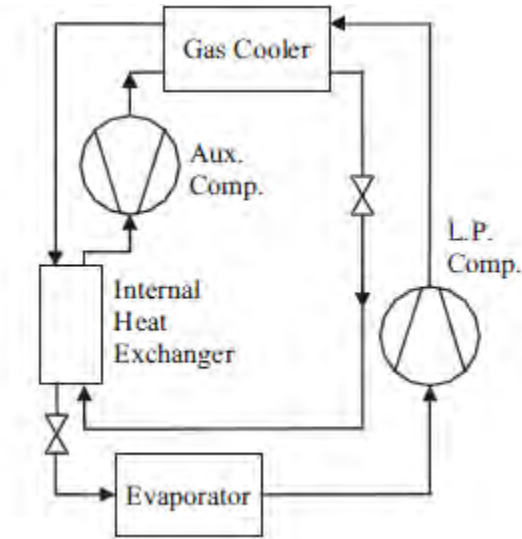


**Figure 12.** Schematic diagram of an auxiliary loop TCHP system

### **2.5.3. Expansion modifications**

The two functions of the expansion device are to maintain the pressure difference between the gas cooler and the evaporator and to maintain proper flow of distribution to the evaporator. Optimum system performance requires maintaining the optimum pressure in the gas cooler; therefore the expansion device plays an important role efficient system operation. The basic cycle include expansion through an expansion valve, but there are also many ways that are being used for refrigerant's expansion and we are going to analyze them below.

#### **2.5.3.1. Capillary tubes**

An important modification for the expansion of a transcritical cycle of CO<sub>2</sub> system constitutes the use of capillary tubes. Small refrigeration and heat pump units using conventional refrigerants commonly incorporate capillary tubes for expansion control, but there has been uncertainty about the effectiveness of capillary tubes in transcritical CO<sub>2</sub> systems. There have been numerous studies ensuring that a capillary tube can maintain the optimum gas cooler

pressure and achieve optimal overall system performance and generally indicate capillary tubes can perform adequately in transcritical CO<sub>2</sub> heat pump systems.

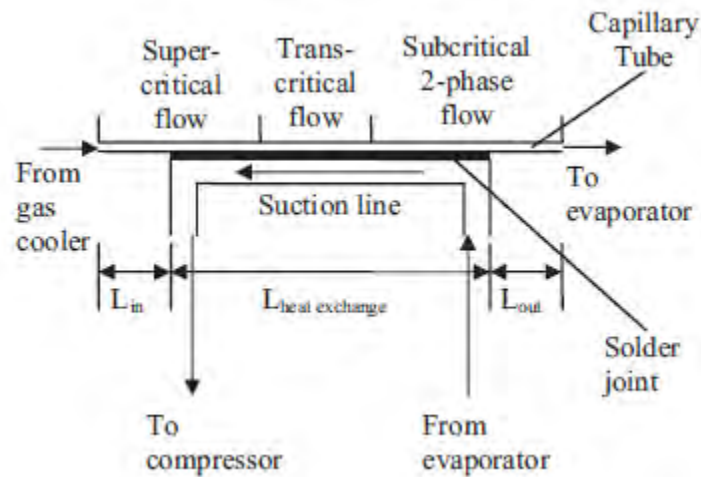


**Figure 13.** Section of a non-adiabatic capillary tube heat exchanger [11]

In the capillary tube, the liquid is expanding from the gas cooler pressure to the evaporation pressure and divided into three fractions: Supercritical flow, which is transmitted, in the capillary tube, gradually to transcritical flow and finally to subcritical two-phase flow, as shown in Figure 13. Therefore, in the transcritical region the fluid is considered as subcooled liquid. In the supercritical and transcritical single-phase region, temperature does not remain constant unlike subcritical refrigeration cycle due to unique shape of temperature lines. As a result, density is not constant giving rise to compressible flow in the entire length of the capillary.

Total tube length is expressed as:  $L = L_{sup} + L_{subliq} + L_{tp}$ . The expansion process from point 1 to 4 is shown in Figure 14 on the pressure–enthalpy plane cycle plot. The capillary tube flow model is developed employing the following assumptions:

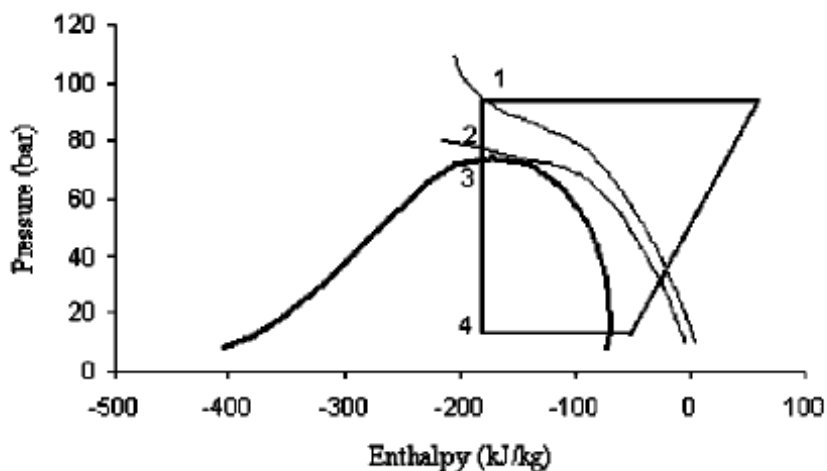


**Figure 14.** P-h diagram of TCHP with expansion through capillary tube

- Straight tube with constant inner diameter and roughness.
- Homogeneous and one-dimensional flow through the tube.
- Flow is adiabatic with no work done.
- Thermodynamic equilibrium prevails in the system.
- Refrigerant is free of oil.
- Flow through the tube is fully developed turbulent flow.
- Entrance losses are negligible.

The model is set around fundamental equations of conservation of mass, energy and momentum and it incorporates variation in property values. This latter feature is essential for simulation of transcritical CO<sub>2</sub> system as property variation is extremely large closely to the critical point. The subsequent parametric study includes the effect of various design parameters, namely, tube diameter, tube relative roughness and refrigerant flow rate. The capillary tube is discretized into a number of longitudinal elements to enable the sharp changes in CO<sub>2</sub> property to be included in the analysis.

### **2.5.3.2. Expansion work recovery**

Using an expansion valve or capillary tube results in an energy loss because no useful work is done by the expansion process. These expansion losses associated with heat pumps using conventional refrigerants are generally small. In a transcritical CO<sub>2</sub> cycle, the greater pressure difference results in greater expansion losses, thus making work recovery more feasible and more beneficial and improving COP. Enthalpy decreases in expansion process and hence the net work requirement reduces and cooling effect increases, which will improve the COP of the cycle.

There are many devices which can potentially be used as expanders for the purpose of work recovery in a TCHP. In addition to turbines (Figure 15), expander types include rotary, reciprocating, scroll, screw, and vane. Each design has its advantages and limitations. Experimental and theoretical research has been conducted on a wide variety of systems and this by Robinson and Groll [7] has shown that work recovery turbine with isentropic efficiency of 60%, may reduce contribution to total irreversibility by about 35% and cause an average increase of COP by 25%.

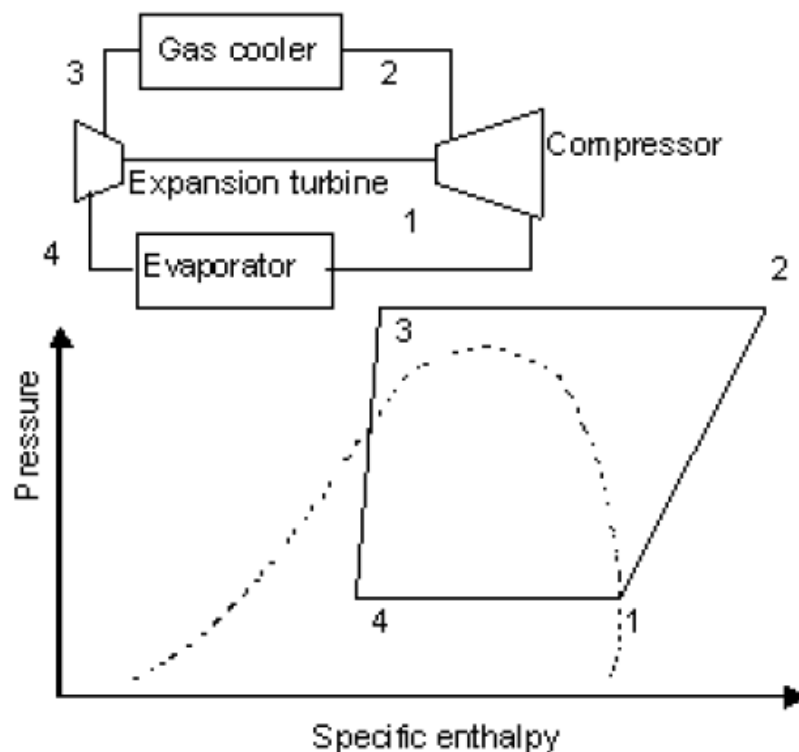


**Figure 15.** Schematic diagram and P-h diagram of transcritical CO<sub>2</sub> system with expansion turbine [6]

### 2.5.3.3. Ejector- expansion

An alternative method to reduce expansion losses in a transcritical CO<sub>2</sub> cycle, is the use of an ejector, by regenerating expansion energy and increasing refrigerant pressure by means of an ejector is an effective way to improving the COP. In addition, the ejector simplifies the process of controlling the gas cooling pressure in the CO<sub>2</sub> cycle. An ejector reduces expansion losses and also increases the pressure at the compressor inlet, thus reducing compressor work. Figure 16 shows the schematic diagram and corresponding P–h diagram of a typical ejector cycle. The basic principles of ejector cycle are as follows. The gas cooling pressure of the CO<sub>2</sub> cycle could be controlled by changing the throat area of ejector nozzle, so high pressure CO<sub>2</sub> from the gas cooler enters the nozzle of the ejector where its velocity is increased and pressure is decreased. In ejector expansion refrigeration cycle, the primary flow from the gas cooler (state 3) and the secondary flow from the evaporator (state 8) are going through primary and secondary nozzles, respectively, constant pressure/area mixing chamber (p-h diagram of CO<sub>2</sub> cycle with constant pressure mixing ejector is shown Figure 16b) and diffuser (10-5) of the ejector. CO<sub>2</sub> then enters a liquid–vapor separator and then separated in forms of vapor (state 1), from which vapor is drawn into the compressor, and liquid (state 6), which re-enters the evaporator, so that this

ratio should be matched with the inlet ratio of primary and secondary flows. Then the liquid circulates through expansion valve (6-7) and evaporator (7-8), whereas the vapor circulates through compressor (1-2) and gas cooler (2-3).

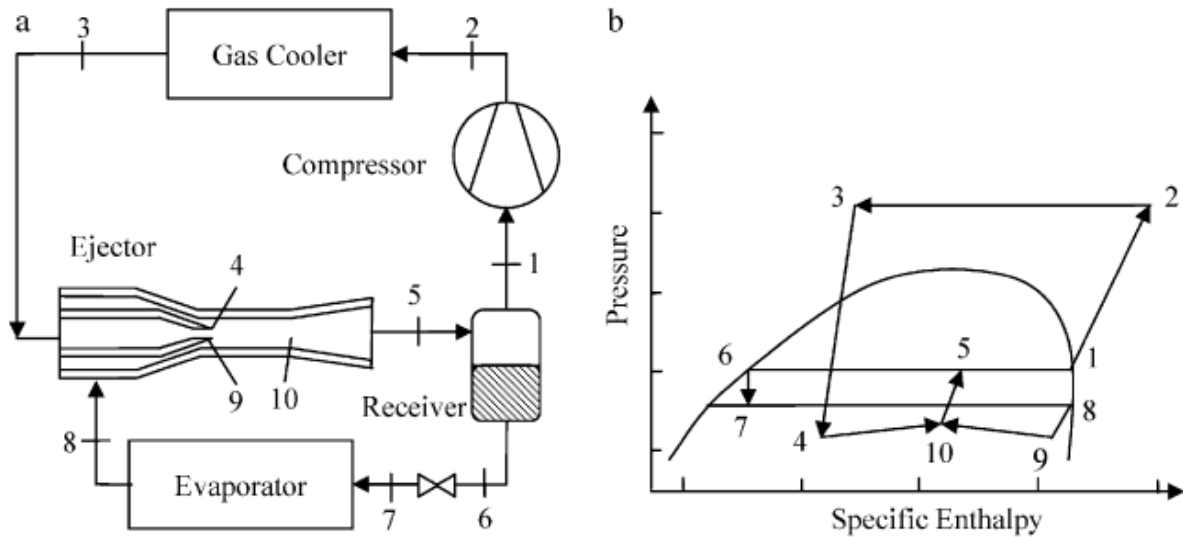


**Figure 16.** Transcritical CO<sub>2</sub> system with ejector expander: (a) Schematic diagram, (b) P-h diagram [1]

Three ejector parameters, entrainment ratio, pressure lift ratio and geometric area ratio significantly influence the system performance with an optimum ratio. The use of an ejector in a transcritical CO<sub>2</sub> cooling cycle was theoretically and experimentally analyzed and many studies have found significant improvements in COP.

### 3. Modeling of transcritical CO<sub>2</sub> heat pump systems

Modeling of a transcritical carbon dioxide heat pump system is conducted based on thermodynamic analysis of the system and based on the transport characteristics of the refrigerant and the secondary fluid (usually water or air). The entire system has been modeled based on energy balance of individual components yielding conservation equations. To consider the lengthwise property variation, all the heat exchangers have been discretized and momentum and energy conservation equations have been applied to each segment. Model analysis, as has been presented in numerous studies [12-17], includes some simplified assumptions, as the following:

- The system is operating at steady state
- Changes in kinetic and potential energies are negligible
- Compression process is adiabatic
- All heat exchangers operate adiabatically
- Heat loss in connecting piping is negligible
- Pressure drop on waterside and in connecting pipes is negligible
- Refrigerant is free from oil
- The expansion process is isenthalpic

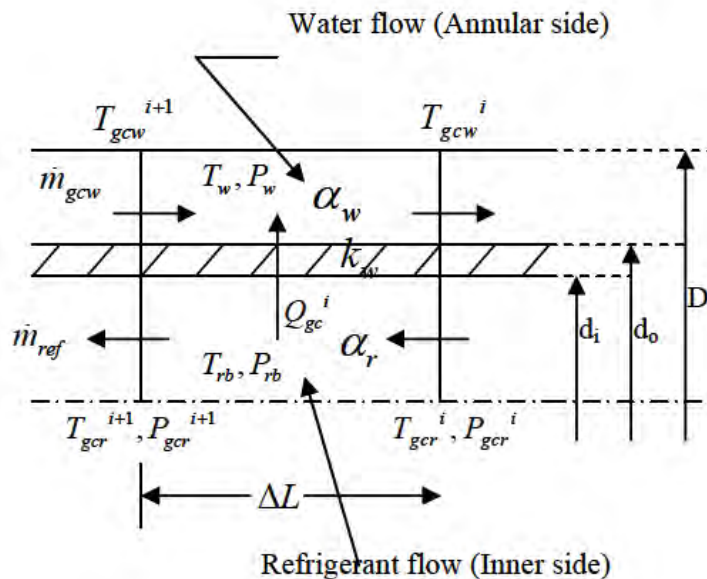


Figure 17. A computational segment of heat exchangers

### 3.1. Thermodynamic analysis

Heat pump performance is generally analyzed in terms of heating capacity and coefficient of performance (COP). Heating capacity is the amount of heat that is being exchanged in the heat exchangers and delivered to the secondary fluid or is being absorbed from this one and imparted to refrigerant. It is calculated as shown in Equation (3), where  $\dot{m}$  is the refrigerant mass flow rate and  $h_i$  and  $h_o$  are the refrigerant enthalpy values at the heat exchanger inlet and outlet respectively.

$$Q = \dot{m}(h_i - h_o) \quad (3)$$

Coefficient of performance (COP) can be defined in terms of heating (the ratio of heat output to compressor work) or cooling (the ratio of heat removed over compressor work)

$$COP_{heating} = \frac{Q_{gc}}{W_{comp}} = \frac{h_{gc,i} - h_{gc,o}}{h_{comp,o} - h_{comp,i}} \quad (4)$$

$$COP_{cooling} = \frac{Q_{ev}}{W_{comp}} = \frac{h_{ev,o} - h_{ev,i}}{h_{comp,o} - h_{comp,i}} \quad (5)$$



Figure 18. A photograph of ground source CO2 air conditioning and heat pump system [18]

### 3.1.1. Gas Cooler

The gas cooler is typically modeled as a double-tube counter flow heat exchanger where the refrigerant flows through the inner tube and water flows through the outer annular space (Figure 19). Energy balance equations can be defined for both the refrigerant side and the water side as shown below:

$$Q_{gc} = \dot{m}_{gc} (h_{gc,i} - h_{gc,o}) \quad (6)$$

$$Q_{gc} = \dot{m}_w c_{p,w} (T_{gc,w,o} - T_{gc,w,i}) \quad (7)$$

Heat transfer in a concentric tube gas cooler is generally considered to occur only in the radial direction and heat transfer along the tubes is negligible. The temperature gradient along the tubes is much greater in a gas cooler than in a conventional condenser or evaporator. This has raised some question as to the suitability of assuming negligible longitudinal heat transfer, but it has been approved that even in the regions with the greatest temperature gradient, the impacts of longitudinal heat flow in gas cooler tubes is negligible and that's what was assumed in this thesis.

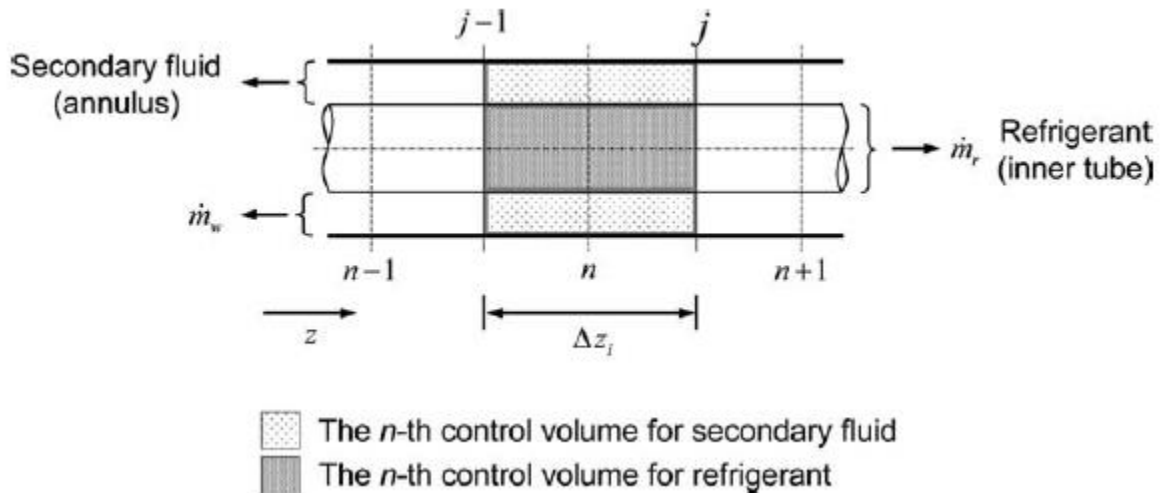


**Figure 19.** Discretization of a double-tube counter flow gas cooler

The heat transfer rate,  $Q_{gc}$ , can be defined based on the overall heat transfer coefficient and the temperature difference between the two fluids. Heat transfer rate is calculated in Equation

(8) using the logarithmic mean temperature difference method (LMTD) (Equation (9)) for heat exchangers. In Equation (8)  $U$  is the overall heat transfer coefficient and  $A$  is the heat transfer area.

$$Q_{gc} = UA \cdot LMTD \quad (8)$$

$$LMTD = \frac{(T_{gc,i} - T_{gc,w,o}) - (T_{gc,o} - T_{gc,w,i})}{\ln \frac{(T_{gc,i} - T_{gc,w,o})}{(T_{gc,o} - T_{gc,w,i})}} \quad (9)$$

Gas cooler as heat exchanger, uses a secondary fluid in order to cool the refrigerant. The energy balance in gas cooler with respect to external fluid being heated:

$$\dot{m}_{gc,w} c_{p,gc,w} \Delta T_{gc,w} = \dot{m}_{ref} q_{gc} \quad (10)$$

### **3.1.2. Evaporator**

Making just the same considerations as for gas cooler, we can express energy balances for evaporator with the following relationships:

$$Q_{ev} = \dot{m} (h_{ev,o} - h_{ev,i}) \quad (11)$$

$$Q_{ev} = \dot{m}_w c_{p,w} (T_{ev,w,i} - T_{ev,w,o}) \quad (12)$$

$$Q_{ev} = UA \frac{(T_{ev,w,i} - T_{ev,o}) - (T_{ev,w,o} - T_{ev,i})}{\ln \frac{(T_{ev,w,i} - T_{ev,o})}{(T_{ev,w,o} - T_{ev,i})}} \quad (13)$$

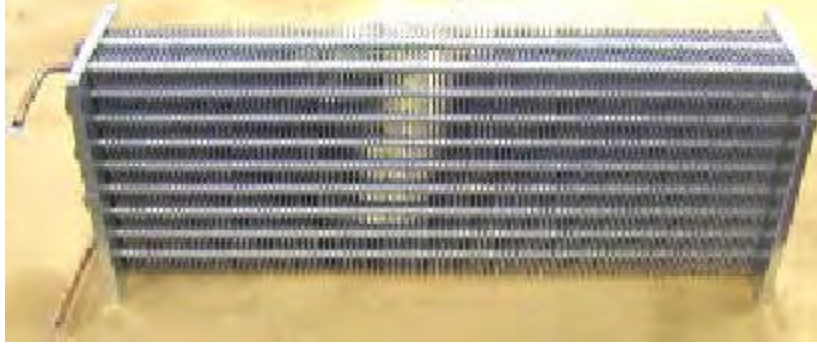


**Figure 20.** Evaporator

For the two heat exchangers, gas cooler and evaporator, there is an alternative computation method for the heat capacity that is being interchanged. In heat exchanger analysis, when there is insufficient information to calculate the LMTD, the NTU or the Effectiveness ( $\epsilon$ ) method is used. The calculations for this method take place with the following equations:

$$\epsilon = \frac{1 - e^{[-NTU(1-R)]}}{1 - c_{\min} e^{[-NTU(1-R)]}} \quad (14)$$

where

$$NTU = \frac{UA}{c_{p,\min}} \quad (15)$$

$$R = \frac{c_{p,\min}}{c_{p,\max}} \quad (16)$$

And just like in LMTD method, we have:

$$\frac{1}{UA} = \frac{1}{h_r A_r} + \frac{\ln(d_o/d_i)}{2 \cdot \pi \cdot \Delta L \cdot k_w} + \frac{1}{h_w A_w} \quad (17)$$

Evaporator is a heat exchanger, so we have also a secondary fluid. The energy balance in evaporator with respect to external fluid being cooled:

$$\dot{m}_{ev,w} c_{p,ev,w} \Delta T_{ev,w} = \dot{m}_{ref} q_{ev} \quad (18)$$

### 3.1.3. Compressor

The transcritical CO<sub>2</sub> refrigeration cycle has high operation pressure. Also, the pressure ratio in the transcritical CO<sub>2</sub> refrigeration cycle is rather low, while the pressure difference is high compared to conventional HFCs' refrigeration cycle.

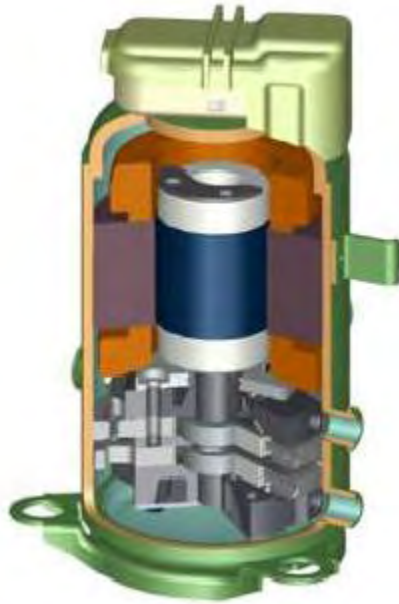


Figure 21. CO<sub>2</sub> compressor

With the assumption that the compressor is operating adiabatically, the compressor work can be calculated as:

$$\dot{W}_{comp} = \frac{\dot{m}}{\eta_{is}} \times (h_{discharge,is} - h_{suction}) = \frac{\dot{m}(h_{2,is} - h_1)}{\eta_{is}} \quad (19)$$

The mass flow rate ( $\dot{m}$ ) can be related to compressor operation as defined in Equation (20) and is considered constant in every component.

$$\dot{m}_{ref} = \rho_{suction} \cdot \eta_V \cdot V_s \cdot \frac{N}{60} \quad (20)$$

Where

$V_s$  :  $V_{swept}$  is the swept volume of the compressor

$\eta_V$  : the volumetric efficiency of the compressor

N: the compressor speed

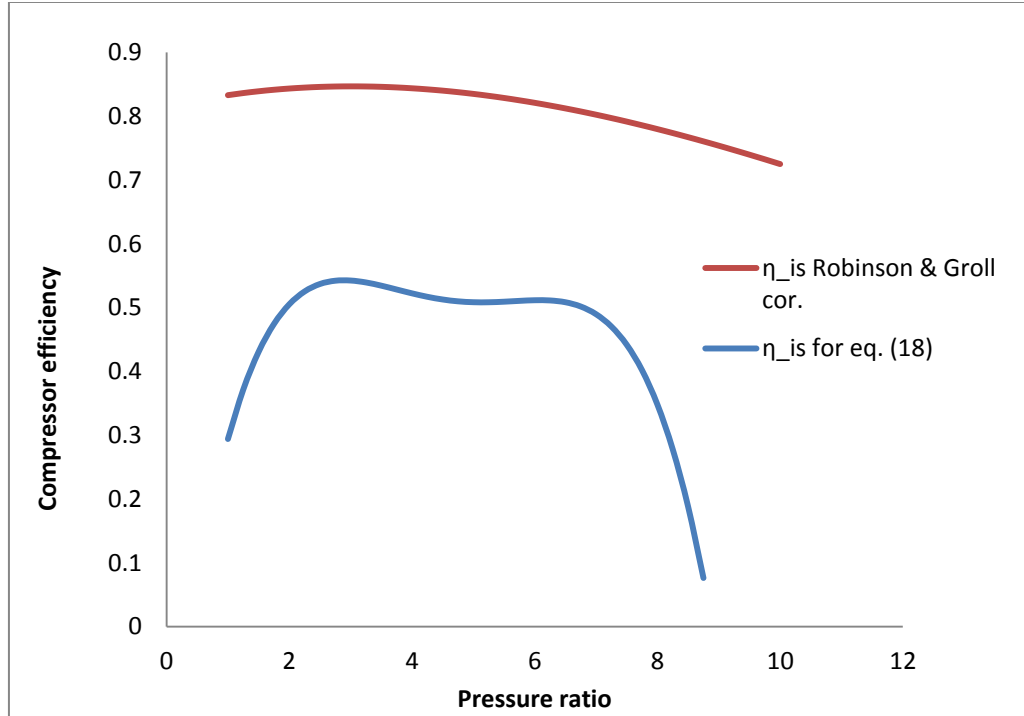
$\rho_{suction}$  : the density of the refrigerant at the suction

The volumetric and isentropic efficiencies are both functions of the compressor pressure ratio ( $PR_c = \frac{P_{dis}}{P_{suc}}$ ) and can be estimated by the correlation given in Equation (21) and (22) [19].

$$\eta_V = 0.9207 - 0.0756 \left( \frac{P_{dis}}{P_{suc}} \right) + 0.0018 \left( \frac{P_{dis}}{P_{suc}} \right)^2 \quad (21)$$

$$\eta_{is,c} = -0.26 + 0.7952 \left( \frac{P_{dis}}{P_{suc}} \right) - 0.2803 \left( \frac{P_{dis}}{P_{suc}} \right)^2 + 0.414 \left( \frac{P_{dis}}{P_{suc}} \right)^3 - 0.0022 \left( \frac{P_{dis}}{P_{suc}} \right)^4 \quad (22)$$

It has been assumed that the compressor that is used is semi-hermetic and the volumetric and isentropic efficiencies have been proposed according to experimental data. In bibliography, there are studies that propose a different correlation for compressor's isentropic efficiency, but our results will be presented with the correlation given in Equation (22). Below is presented the difference with the correlation for compressor's efficiency proposed by Robinson and Groll [7].



**Graph 1.** Plot of isentropic compressor efficiency versus pressure ratio using equation (22) and correlation proposed by Robinson & Groll [7]

### 3.1.4. Expansion device

The energy balance for the expansion device, when it is used an expansion valve, is being modeled as isenthalpic. Of course, it has to be changed when we modify the expansion procedure with expansion recovery or other way of expansion, as capillary tubes.

$$h_{exp,i} = h_{exp,o} \quad (23)$$

During this thesis, apart from expansion valve, the use of turbine for expansion work recovery was modeled and the equations that govern its performance are defined below:

$$w_{turb} = h_{out} - h_{in} - q_{t,loss} \quad (24)$$

And if we take account the compressor's work, we have to use the net work, as

$$W_{net} = W_{turb} - W_{comp} \quad (25)$$

### **3.1.5. Internal heat exchanger**

The internal heat exchanger is a component that is not included in the basic cycle's components, but is an addition to ensure vaporization of the refrigerant before its compression, in order to reduce power input to the compressor, as it has been discussed in 2.5.1. The energy balance for the internal heat exchanger is:

$$h_{gc,out} - h_{exp,in} = h_{comp,in} - h_{ev,out} \quad (26)$$

## **3.2. Transport characteristics of CO<sub>2</sub>**

In order to develop our numerical model, it was very necessary to use the accurate correlations relative to CO<sub>2</sub>'s behavior over supercritical and subcritical regions, according to available bibliography. In the subcritical and supercritical flow regions, the magnitude and variation of transport properties of CO<sub>2</sub> (viscosity and thermal conductivity) and other properties differ significantly relatively to other fluids. As consequence, well established correlations that govern effects which relate the heat transfer coefficient and pressure drop under different conditions are inaccurate for CO<sub>2</sub>. In order to create sufficient numerical models of transcritical heat pump systems using CO<sub>2</sub>, it was indispensable to use accurate correlations to predict the heat transfer coefficient and pressure drop during supercritical gas cooling, single phase heating and cooling, and flow boiling processes.

### 3.2.1. Supercritical cooling (Gas-cooler Analysis)

#### 3.2.1.1. Heat transfer correlations

In supercritical region, many of the properties of carbon dioxide depending on temperature and pressure change drastically with the variation of these variables. Property variation is more significant in a region near the pseudo critical temperature. The pseudo critical temperature ( $T_{pc}$ ) is defined as the temperature at which the specific heat of  $CO_2$  reaches a maximum. We can compute  $T_{pc}$  of  $CO_2$  with Equation (27), which is proportional to the pressure condition [1].

$$T_{pc} = -31.40 + 12.15P - 0.6297P^2 + 0.0316P^3 + 0.000752P^4 \quad (27)$$

Heat transfer and flow characteristics, such as viscosity, thermal conductivity, specific heat and density, are being affected strongly by the variation in  $CO_2$ 's properties. These variations must be taken into account in heat transfer correlations of supercritical  $CO_2$  during cooling process in the gas cooler. It should be noticed that correlations developed for supercritical heating do not accurately predict the heat transfer during supercritical cooling.

Regarding to heat transfer coefficient for the supercritical region of  $CO_2$ , there are numerous studies that propose different ways to compute the correlation that can predict the experimental results better (Figure 22).

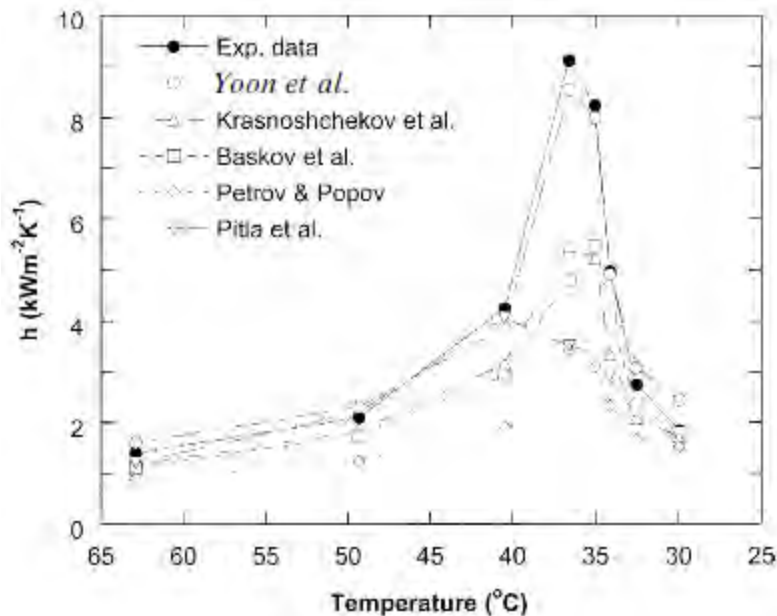


Figure 22. Comparison of experimental data with the calculated heat transfer coefficients using existing correlations as a function of carbon dioxide temperature [20]

The properties variation includes two aspects: variation along the direction of flow and variation perpendicular to the direction of fluid flow. To estimate heat transfer rates, Gnielinski [21] equation, that is used generally for turbulent flow in tubes, is not suitable for normal tube (may be useful for micro-channel) due to large variation of fluid properties in the radial direction. To alleviate this deficiency, Pitla et al. [22] proposed a modification for supercritical in-tube carbon dioxide cooling, incorporating both bulk and wall properties. This correlation, used for gas cooler analysis, is given by:

$$Nu_r = \left( \frac{Nu_{rw} + Nu_{rb}}{2} \right) \frac{k_{rw}}{k_{rb}} \quad (28)$$

$$h_r = \frac{Nu_r}{d_i} k_{rb} \quad (29)$$

Here,  $Nu_{rb}$  and  $Nu_{rw}$  are the Nusselt numbers at bulk and wall temperature respectively, predicted by Gnielinski equation (Equation (30)) within the range  $2300 < Re < 10^6$  and  $0.6 < Pr < 105$ .

$$Nu = \frac{(f/8)(Re-1000)Pr}{1.07 + 12.7(f/8)^{1/2}(Pr^{2/3}-1)} \quad (30)$$

Where  $f$  is the friction factor given by:

$$f = (0.79 \ln(Re) - 1.64)^{-2} \quad (31)$$

The water side heat transfer coefficient ( $h_{water}$ ) is evaluated by the Dittus-Boelter equation for annular flow. All water properties are assumed to be temperature dependent only, and polynomial expressions based on text book values have been used.

$$Nu_D = 0.023 \cdot Re_D^{4/5} Pr^n \quad (32)$$

where:

D is the inside diameter of the circular duct

Pr is the Prandtl number

n=0.4 for heating of the fluid (evaporator), and n=0.3 for cooling of the fluid (gas cooler)

The Dittus-Boelter equation is valid for:

$$0.6 \leq Pr \leq 160$$

$$Re_D \geq 10000$$

$$L/D \geq 10$$

### 3.2.1.2. Pressure drop correlations

The pressure drop for supercritical CO<sub>2</sub> is expressed by the Darcy–Weisback equation, which relates the pressure loss due to friction along a given length of pipe to the average velocity of the fluid flow, for single-phase pressure drop as shown in Equation (33), where f is the friction factor and ξ is the minor loss coefficient.

$$\Delta P = \frac{\rho V^2}{2} \cdot \left( f_D \cdot \frac{L}{D} + \xi \right) \quad (33)$$

The friction factor coefficient can be computed by the following correlations proposed by Blasius or Petrov-Popov.

<b>Blasius</b>	or	$f = \frac{0.316}{Re^{0.25}}$	for $Re \leq 2 \times 10^4$	<b>(34)</b>
		$f = \frac{0.184}{Re^{1/5}}$	for $Re > 2 \times 10^4$	
<b>Petrov-Popov</b>		$f = f_{c,w} \frac{\rho_w}{\rho_b} \left( \frac{\mu_w}{\mu_b} \right)^s$	for $1.4 \times 10^4 \leq Re_w \leq 10^5$	<b>(35)</b>
		$s = 0.023 \left( \frac{ q_w }{G} \right)^{0.42}$	for $3.1 \times 10^4 \leq Re_b \leq 8 \times 10^5$	

**Table 3.** Table for friction factors correlations for pressure drop calculation

Where  $f_{(c,w)} = [1.82 \cdot \ln(Re_{rw}) - 1.64]^{(-2)}$  the friction factor coefficient for constant thermophysical conditions. Although, Cheng et al. [23] concluded that the Blasius equation for friction factor predicts the pressure drop of cooling supercritical CO<sub>2</sub> in both micro- and macro-channels with sufficient accuracy, Sarkar uses the correlation proposed by Petrov-Popov in many studies [13-15, 24, 25] and so does our models that were developed.

### **3.2.2. Flow boiling (Evaporator Analysis)**

The pressure drop and heat transfer characteristics of CO<sub>2</sub> during flow boiling have been analyzed in many research works. The results of the studies have typically concluded that the generalized correlations for pressure drop and heat transfer do not adequately predict the behavior of CO<sub>2</sub>. This has led some authors to develop new predictive correlations specific to CO<sub>2</sub>, intending to predict experimental results and validate the new correlations.

High pressure, very low viscosity and surface tension and near critical operation make the flow boiling heat transfer and pressure drop phenomenon of carbon dioxide distinct from conventional refrigerants. Distinct film breakdown and dry-out phenomena make the majority of the general correlation unusable [26].

In this thesis, the correlation developed by Yoon et al. [27] has been employed to estimate the boiling heat transfer coefficient. The following correlation is proposed to predict critical quality:

$$x_{cr} = 38.27 \cdot Re_l^{2.12} \cdot (1000 \cdot Bo)^{1.64} Bd^{-4.7} \quad (36)$$

Where  $Bo = q/G \cdot h_{fg}$  the boiling number,  $q$  is the heat flux (W/m<sup>2</sup>),  $G$  the mass velocity (kg/m<sup>2</sup>s),  $h_{fg}$  the latent heat of evaporation (J/kg) and  $Bd = g(\rho_l - \rho_g)d_i^2/\sigma$  the Bond number,  $d_i$  the inner of inner tube diameter and  $\sigma$  the interfacial surface.

Yoon et al. [27] proposed the following correlation for the heat transfer coefficient, which has been introduced in the numerical model used for evaporator analysis:

➤ For region  $x < x_{cr}$ :

$$h_{two-phase} = \left[ (S \cdot h_{nb})^2 + (E \cdot h_l)^2 \right]^{1/2} \quad (37)$$

Nucleate boiling heat transfer coefficient:

$$h_{nb} = 55 \cdot \text{Pr}^{0.12} (-\log_{10} \text{Pr})^{-0.55} M^{-0.5} q^{0.67} \quad (38)$$

Where  $M$  is the molecular weight and parameters  $S$  and  $E$  are given as:

$$S = [1 + 1.62 \cdot 10^{-6} E^{-0.69} \text{Re}_l^{1.11}]^{-1} \quad (39)$$

$$E = \left[ 1 + 9.36 \cdot 10^3 \cdot \text{Pr}_l \left( \frac{\rho_l}{\rho_g} - 1 \right) \right]^{0.11} \quad (40)$$

➤ For region  $x \geq x_{cr}$ :

$$h_{\text{two-phase}} = \frac{g_{dry} \cdot h_g + (2\pi - g_{dry}) h_{wet}}{2\pi} \quad (41)$$

Where  $h_{wet}$  is the heat transfer coefficient on the wetted portion of the tube:  $h_{wet} = E \cdot h_l$

$$E = 1 + 3000 \cdot \text{Bo}^{0.86} + 1.12 \left( \frac{x}{1-x} \right)^{0.75} \left( \frac{\rho_l}{\rho_g} \right)^{0.41} \quad (42)$$

Where  $g_{dry}$ , the angle of dry portion is closely related to flow pattern (Figure 23) and is suggested as:

$$\frac{g_{dry}}{2\pi} = 36.23 \cdot \text{Re}^{3.47} \text{Bo}^{4.84} \text{Bd}^{-0.27} \left( \frac{1}{X_{tt}} \right)^{2.66} \quad (43)$$

Referring to  $h_g$  and  $h_l$  are heat transfer coefficients corresponding to saturated liquid and vapor, given by Dittus-Boelter equation that referred above.

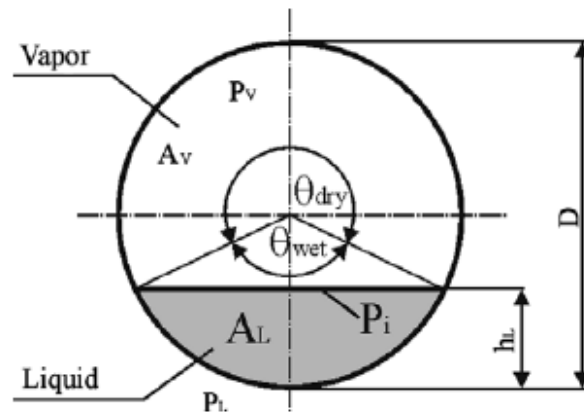


**Figure 23.** Schematic diagram of stratified two-phase flow in a horizontal tube

Pressure drop is being calculated by the modified Martinelli correlation:

$$\Delta P_p = \frac{2f_{fo}G^2L}{d \cdot \rho_l} \left[ \frac{1}{\Delta x} \int_0^x \phi_{tp}^2 dx \right] \quad (44)$$

Where  $f_{fo} = 0.046 \text{Re}^{-0.2}$  and the two phase multiplier is given by:

$$\phi_{tp} = (1-x)^2 + 2.87 \cdot x^2 (P/P_{cr})^{-1} + 1.68x^{0.8} (1-x)^{0.25} (P/P_{cr})^{-1.64} \quad (45)$$

### **3.3. Modeling software tool EES (Engineering Equation Solver)**

Engineering Equation Solver (EES) is a commercial software package, which was developed by two professors, Dr. William Beckman and Dr. Sanford Klein, both of the University of Wisconsin, and is extensively used for solution of systems of simultaneous non-linear equations. It provides many useful specialized functions and equations for the solution of thermodynamics, fluid mechanics and heat transfer problems, making it a useful and widely used program for mechanical engineers working in these fields. EES stores libraries with thermodynamic properties, which eliminates iterative problem solving by hand through the use of code that calls properties from the libraries at the specified thermodynamic properties. EES performs the iterative solving, eliminating the tedious and time consuming task of acquiring thermodynamic properties with its built-in functions, but also with its ready codes for classic thermodynamic cycles and problems. Furthermore, transport properties are also provided for all substances.

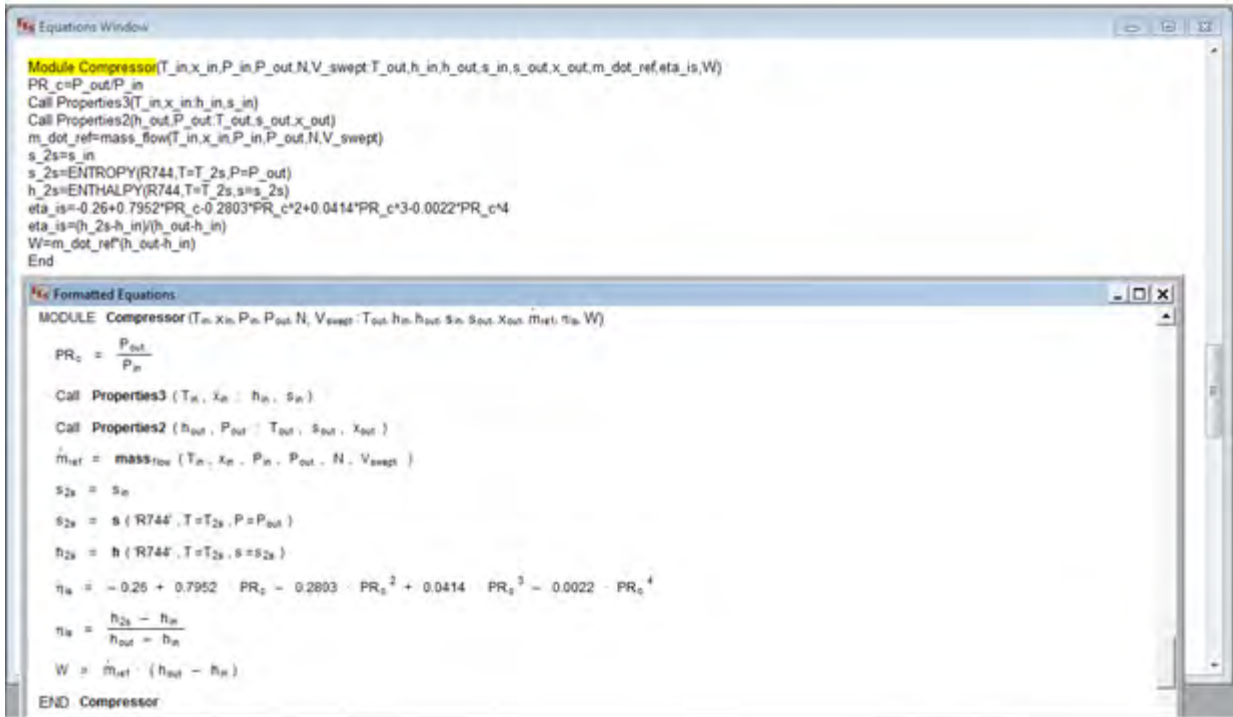


Figure 24. Code and formatted equations from EES

EES also includes parametric tables that allow the user to compare a number of variables at a time. Parametric tables can also be used to generate plots. EES can also integrate, both as a command in code and in tables. EES also provides optimization tools that minimize or maximize a chosen variable by varying a number of other variables. Lookup tables can be created to store information that can be accessed by a call in the code. EES code allows the user to input equations in any order and obtain a solution, but also can contain if-then statements, which can also be nested within each other to create if-then-else statements. Users can write functions for use in their code, and also procedures, which are functions with multiple outputs. Also, compiled functions and procedures, written in a high-level language such as Pascal, C, or FORTRAN, can be dynamically-linked with EES.

Adjusting the preferences allows the user choose a unit system, specify stop criteria, including the number of iterations, and also enable/disable unit checking and recommending units, among other options. Also, it is very important that users can specify guess values and variable limits, from special windows, to aid the iterative solving process and help EES quickly and successfully find a solution.

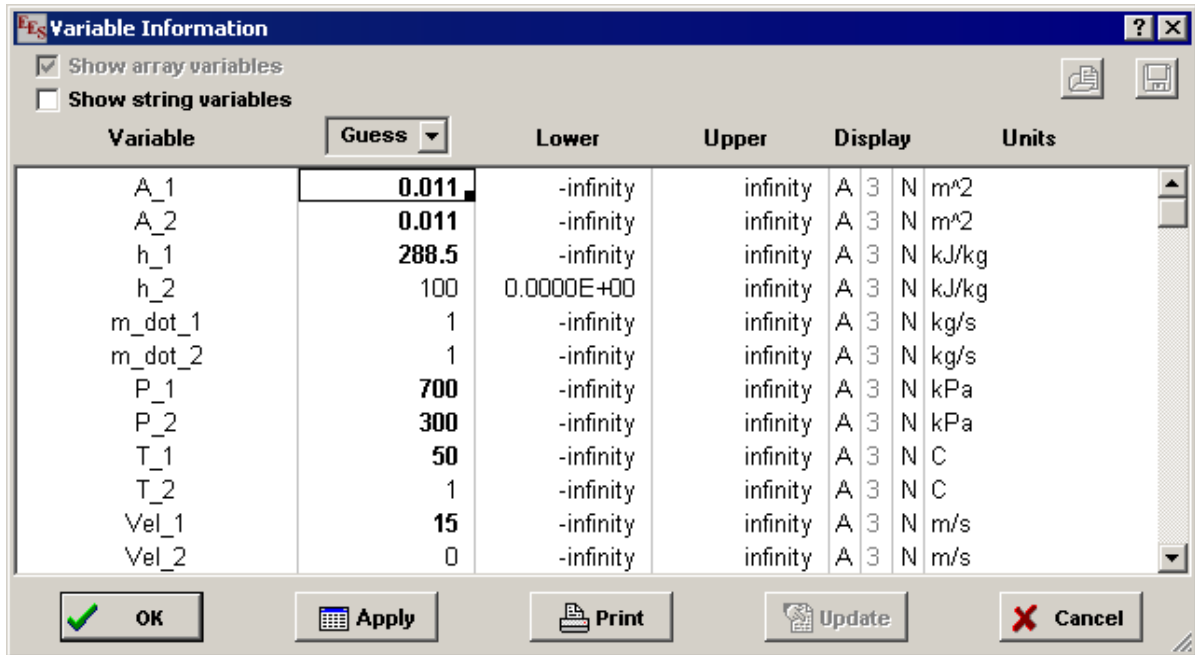


Figure 25. Variable info windows, where we can set guess values and variable limits

So, EES was selected as the most appropriate software tool for modeling the CO<sub>2</sub> transcritical heat pump cycle, in order to avoid building new thermodynamic property libraries, but also for its special property plots that can represent any property diagram easily and quickly, making our task much easier.

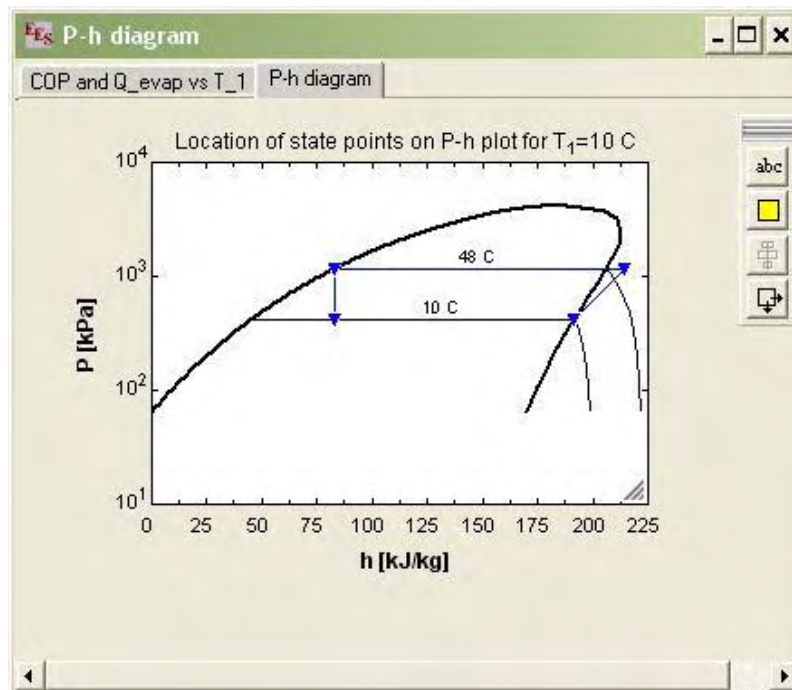


Figure 26. Property plot derived from EES

Furthermore, with the use of this software tool during this thesis, we had the possibility making a parametric study by using the special EES' parametric tables, so we could see the way that  $P_{dis}$  or  $T_{gc,out}$  for example, affects the cooling or heating capacity and subsequently COP, or the relationship between the compressor nominal speed and COP.

The screenshot shows the EES software interface with a parametric table. The table has four columns: a green arrow icon with '1..3', 'N', 'P<sub>2</sub> [bar]', and 'cop'. The rows are labeled 'Run 1' through 'Run 5'. The values for N are 2900, 2500, 2700, 2900, and 2900 respectively. The values for P<sub>2</sub> are 95, 95, 95, 90, and 95. The values for cop are 2.135, 2.423, 2.275, and empty for Run 4 and Run 5.

	1	2	3
	N	P <sub>2</sub> [bar]	cop
Run 1	2900	95	2.135
Run 2	2500	95	2.423
Run 3	2700	95	2.275
Run 4	2900	90	
Run 5	2900	95	

**Figure 27.** Parametric table derived from EES

## 4. Results and discussion

### 4.1. Input parameters and calculation flowchart

It is necessary to refer input parameters that have a very important role for the performance of our system. The following table includes all the components' geometrical parameters, such as inner and outer tubes' length and thickness, but also the input temperature and pressure of the refrigerant and the secondary fluid (water).

Heat exchangers	Gas cooler	Evaporator
Length (m)	14	7.2
Inner tube diameter (mm)	6.35	9.5
Outer tube diameter (mm)	12	16
Inner tube thickness (mm)	0.8	1
Outer tube thickness (mm)	1	1
Tube material	Copper	Copper
<b>Compressor</b>		
Displacement(cm <sup>3</sup> )	11.7	
Nominal speed (rpm)	2900	

**Table 4.** Components specifications

Our model could solve the system either with the outputs temperatures of the evaporator for the water, or with the mass flow (kg/s) of the first and secondary fluid.

Input properties	Values
$T_{\text{water,in,gc}} (^{\circ}\text{C})$	30
$T_{\text{water,out,gc}} (^{\circ}\text{C})$	73
$T_{\text{water,in,ev}} (^{\circ}\text{C})$	30
$T_{\text{water,out,ev}} (^{\circ}\text{C})$	4
$P_{\text{suc}} (\text{kPa})$	$P_{\text{sat}}(T=T_{\text{in}})$
$P_{\text{dis}} (\text{kPa})$	95

**Table 5.** Input properties variables

The system model is composed of each component model by suitable interface parameters coming from the previous component as the input state of the next component and its flowchart is shown in Figure 28. The simplest and most stable solution for system model is a method of successive approximations.

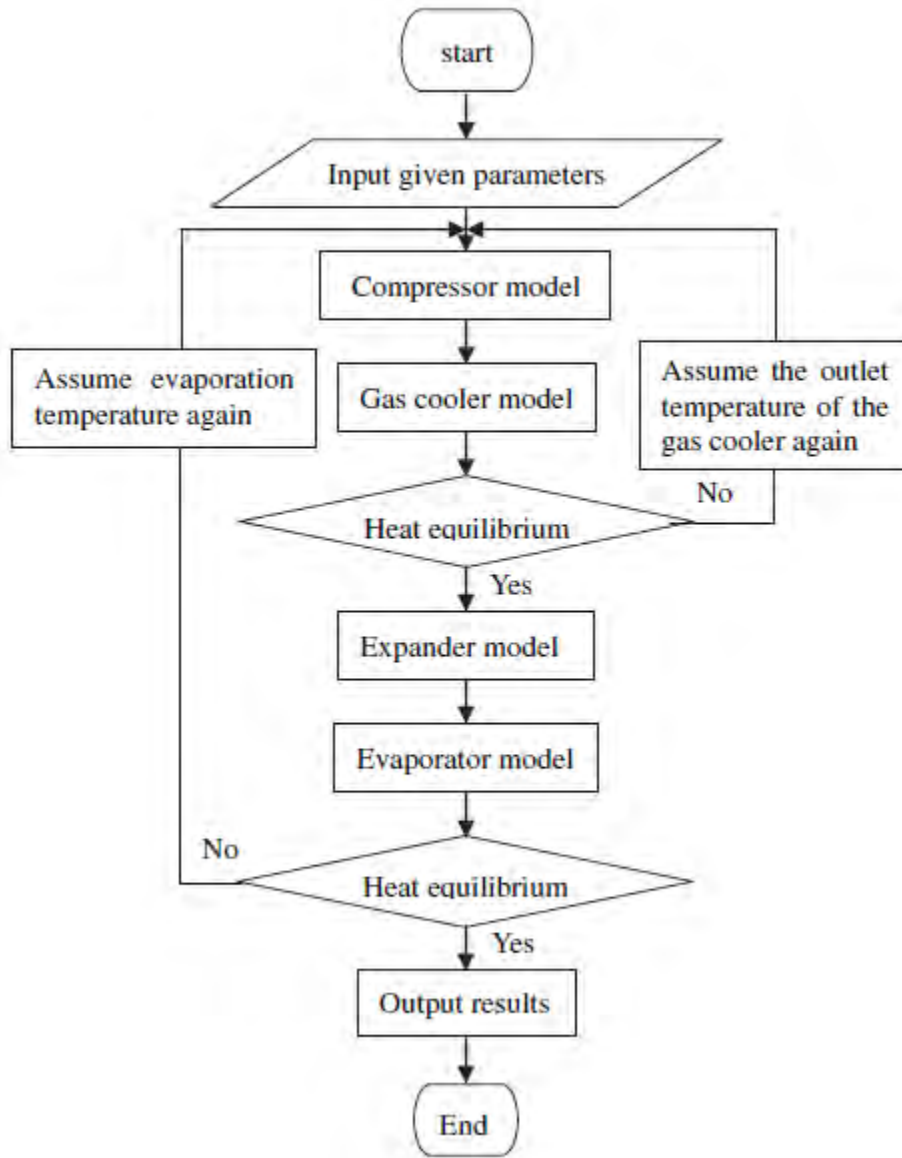


**Figure 28.** Flowchart for the transcritical CO<sub>2</sub> heat pump system

In present thesis, a fixed discharge pressure and guess values for evaporation temperature and gas cooler exit temperature are entered in EES guess values window. The system modeling begins at the inlet to the compressor and runs from the inner loop to the outer loop until the chosen convergence conditions are met. The outputs of the system convergence model are the

final values of all component energy transfer rates including compressor power, gas cooler capacity, expander's power (if a turbine is used) and evaporator capacity. Also, COP (coefficient of performance) for heating and cooling applications is an output of this model.

#### 4.2. Basic TCHP model

The basic transcritical CO<sub>2</sub> heat pump cycle includes a compressor (1→2), a gas-cooler (2→3), an expansion valve (3→4) and an evaporator (4→5), but not an internal heat exchanger, as it is referred earlier.

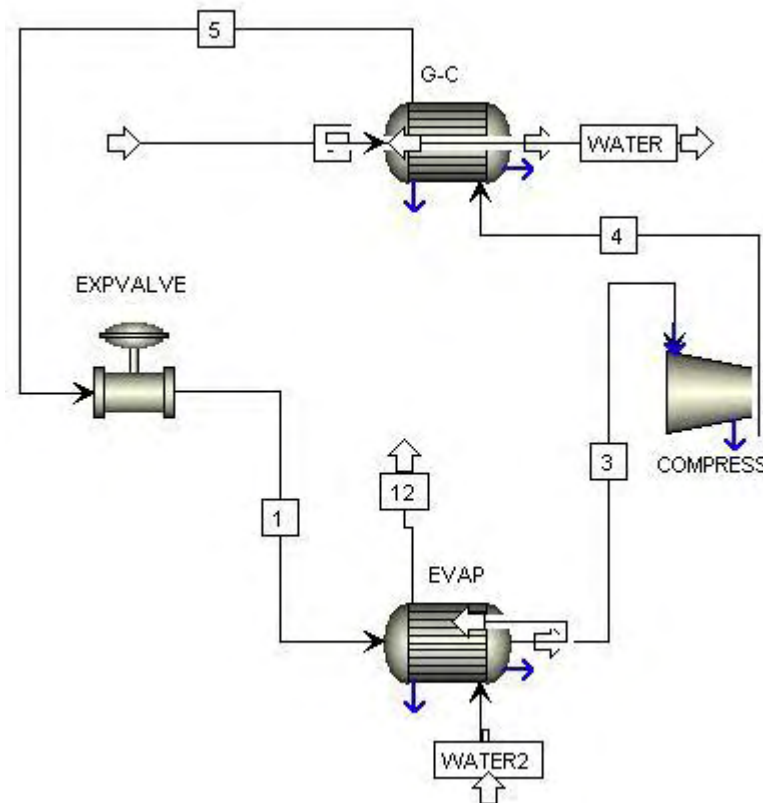


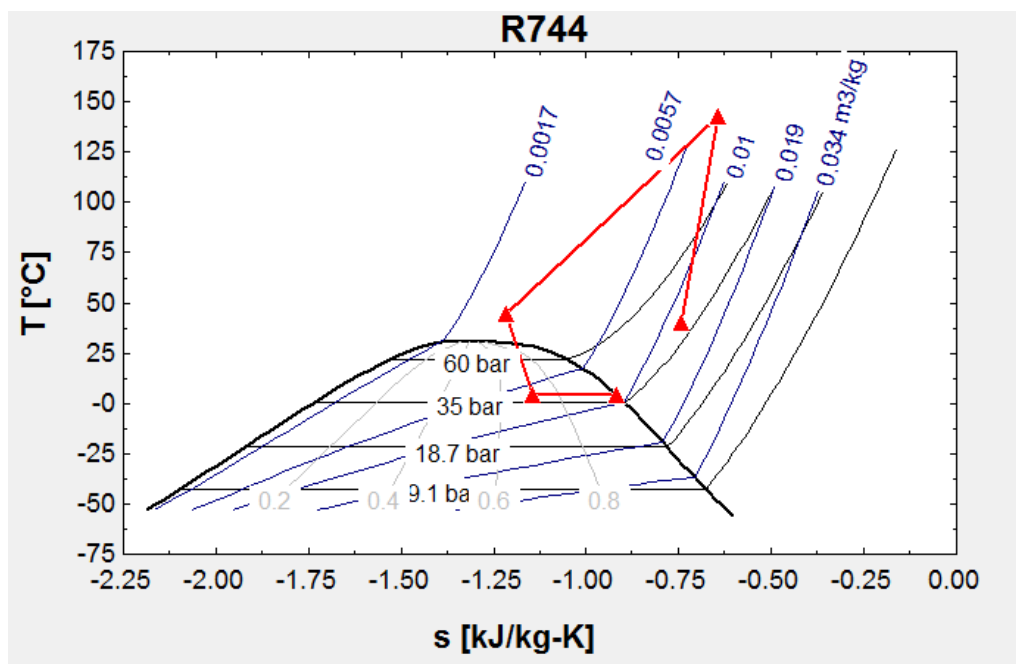
**Figure 29.** TCHP without IHEX designed with ASPEN

The Table 6 contains the values of properties for each stage and the situations 7, 8 and 9, 10 refer to the temperature of water at inlet and outlet of gas cooler and evaporator respectively.

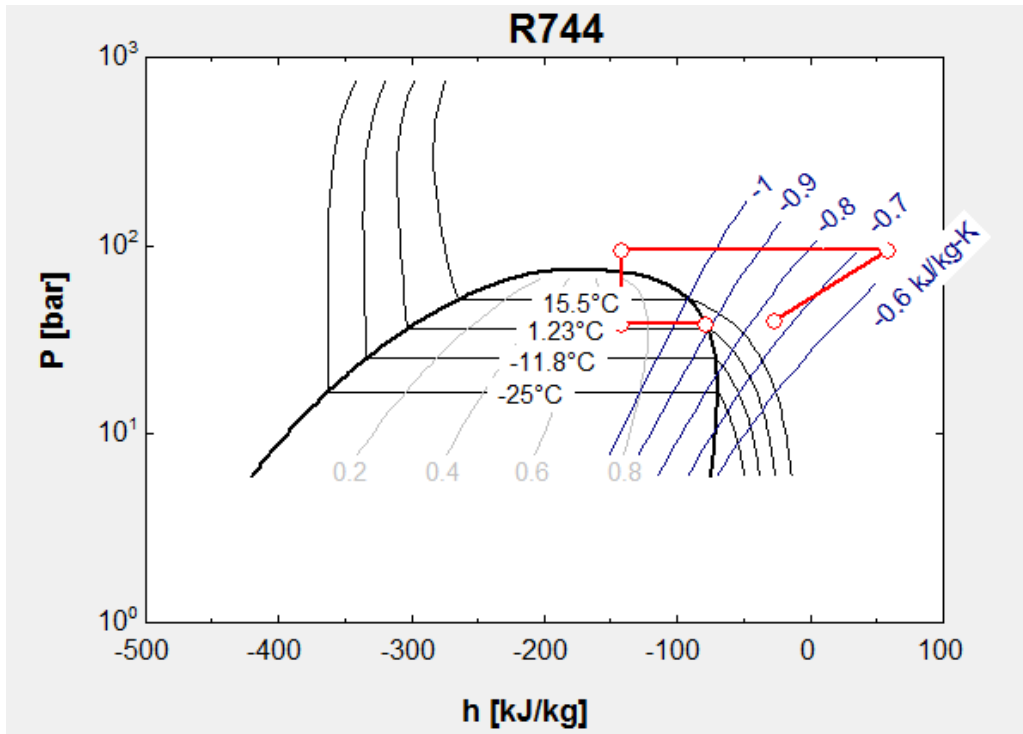
	1	2	3	4	5
	$T_i$ [C]	$P_i$ [bar]	$h_i$ [kJ/kg]	$s_i$ [kJ/kgK]	$x_i$
[1]	40	40	-26.68	-0.7447	100
[2]	142.9	95	58.8	-0.6448	100
[3]	44.54	95	-141.8	-1.215	100
[4]	4	38.69	-141.8	-1.145	0.7099
[5]	4	38.69	-78.53	-0.9167	1
[6]					
[7]	37				
[8]	129.3				
[9]	30				
[10]	5				

**Table 6.** Table with properties values as model output

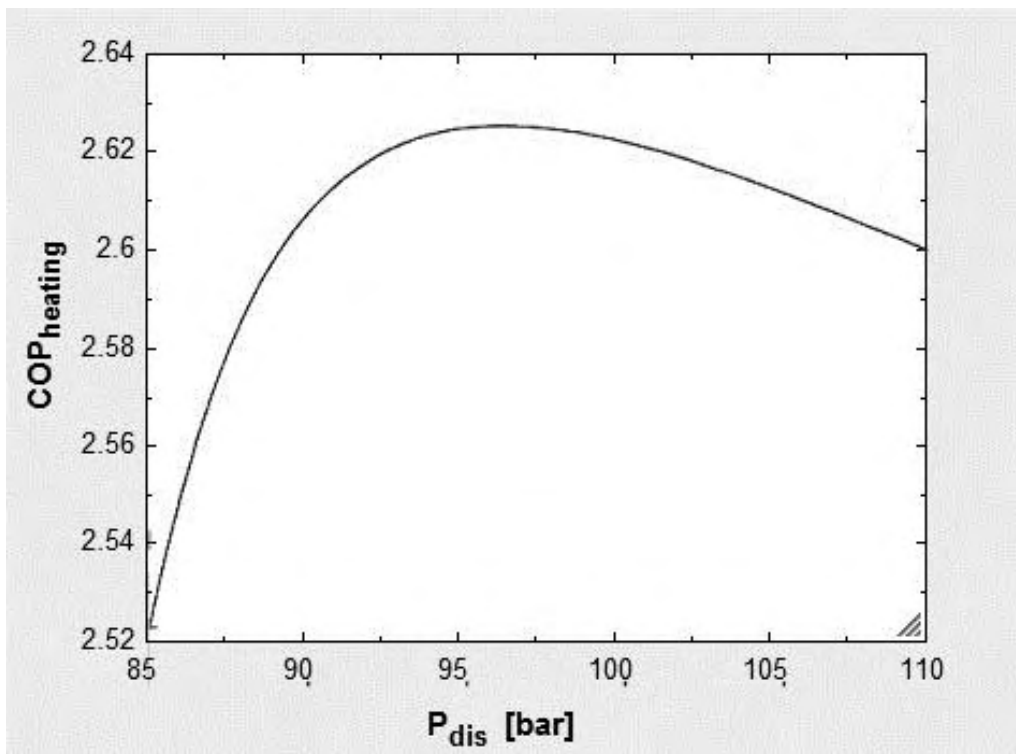
Below we can see the temperature-entropy (T-s) and pressure-enthalpy (P-h) diagrams that result from the basic TCHP model from Table 6. As we can observe, the quality after expansion ( $x_4$ ) is quite large, so the graph is located towards the curve of vaporization.



**Graph 2.** T-s diagram of TCHP model

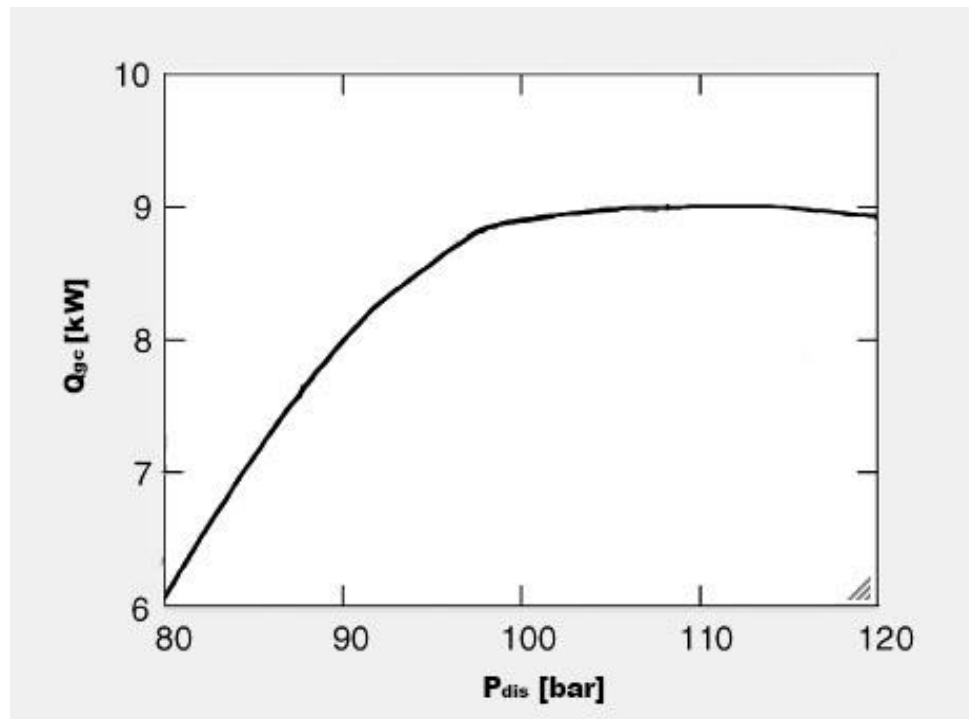


**Graph 3.** P-h diagram of TCHP model



**Graph 4.** COP vs discharge pressure

Maximum COP for heating was equal to 2.64 and it was founded at a discharge pressure about 100-110 bar. Also, it is observed that after this discharge pressure, COP reduces again. Moreover, we can see that how heating capacity ( $\dot{Q}_{gc}$ ) is changing as discharge pressure is increasing. It is observed that there is a maximum  $\dot{Q}_{gc}$  at about 100 bar and after this value heating capacity is reducing as discharge pressure is increasing.



**Graph 5.** Heating capacity variation over discharge pressure

### 4.3. TCHP model with internal heat exchanger (IHEX)

The next model that was developed and studied was the classic transcritical CO<sub>2</sub> heat pump cycle, but with the addition of an internal heat exchanger, with the following alternations in the cycle that have been discussed in chapter 2.5.1.

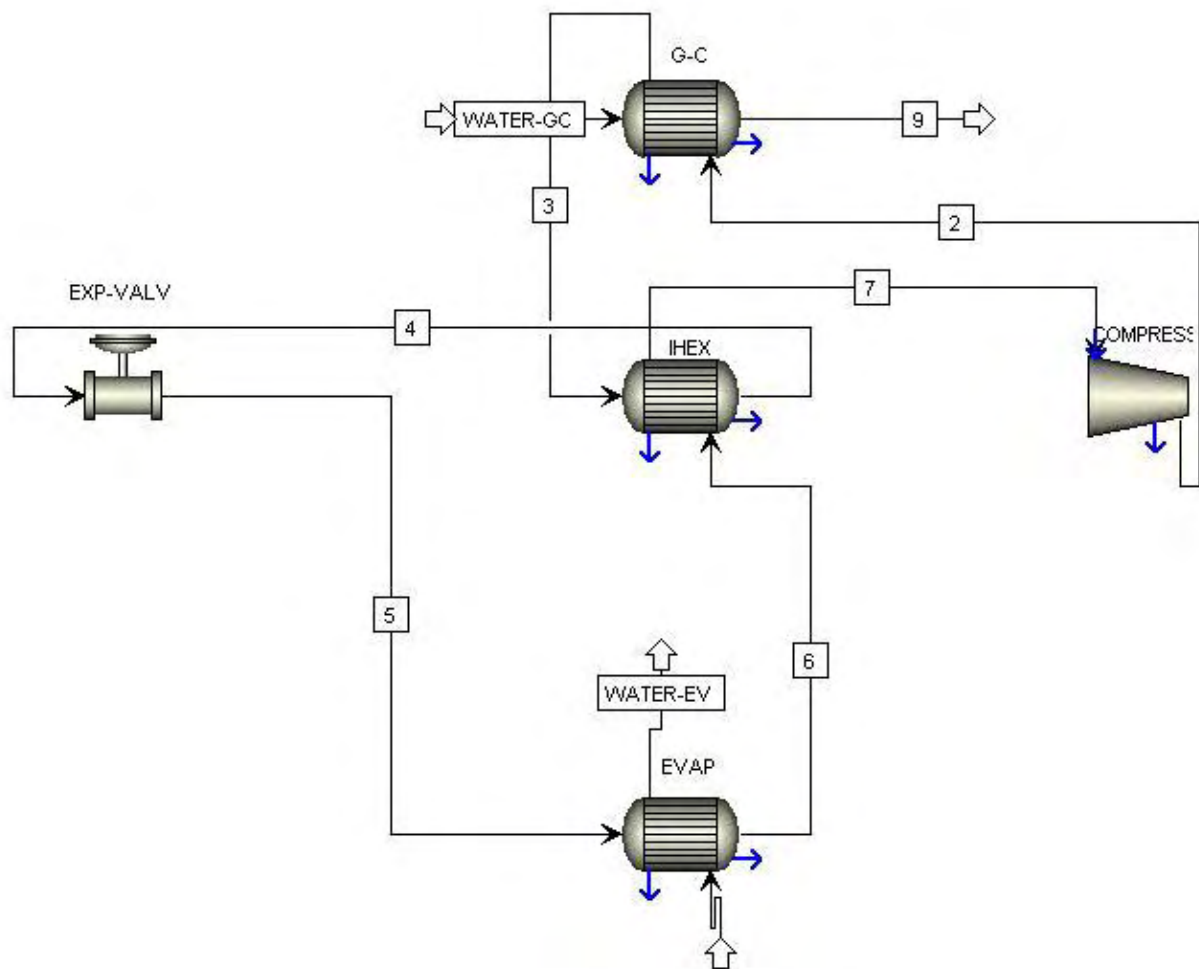


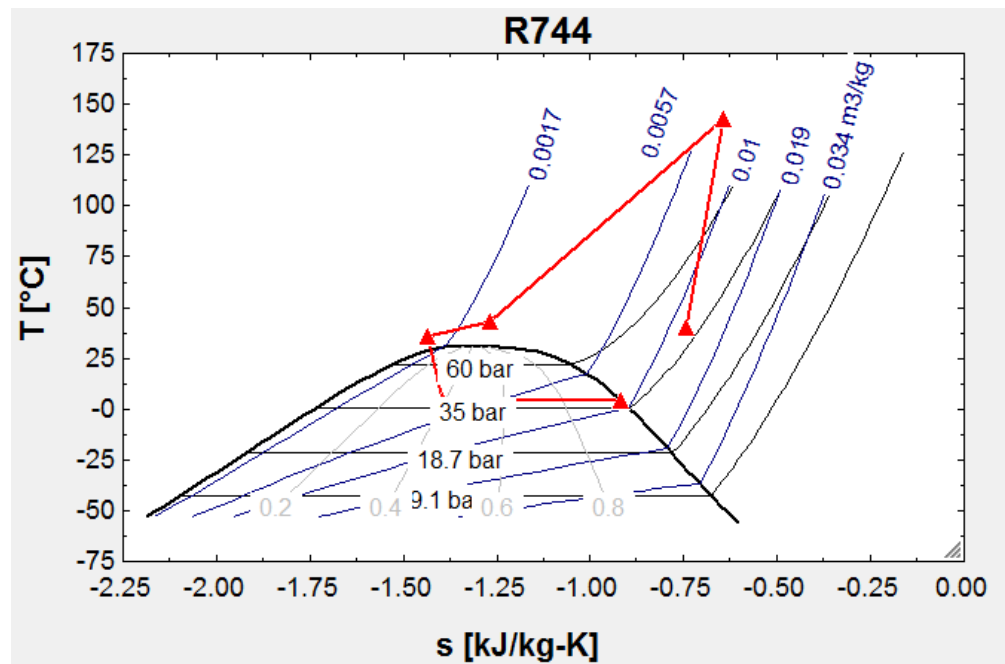
Figure 30. TCHP with IHEX designed with ASPEN

So, the stages are for compressor (1→2), gas-cooler (2→3), internal heat exchanger (3→4), expansion valve (4→5) and an evaporator (5→6). The Table 7 contains the values of properties for each stage and the situations 7, 8 and 9, 10 refer to the temperature of water at inlet and outlet of gas cooler and evaporator respectively.

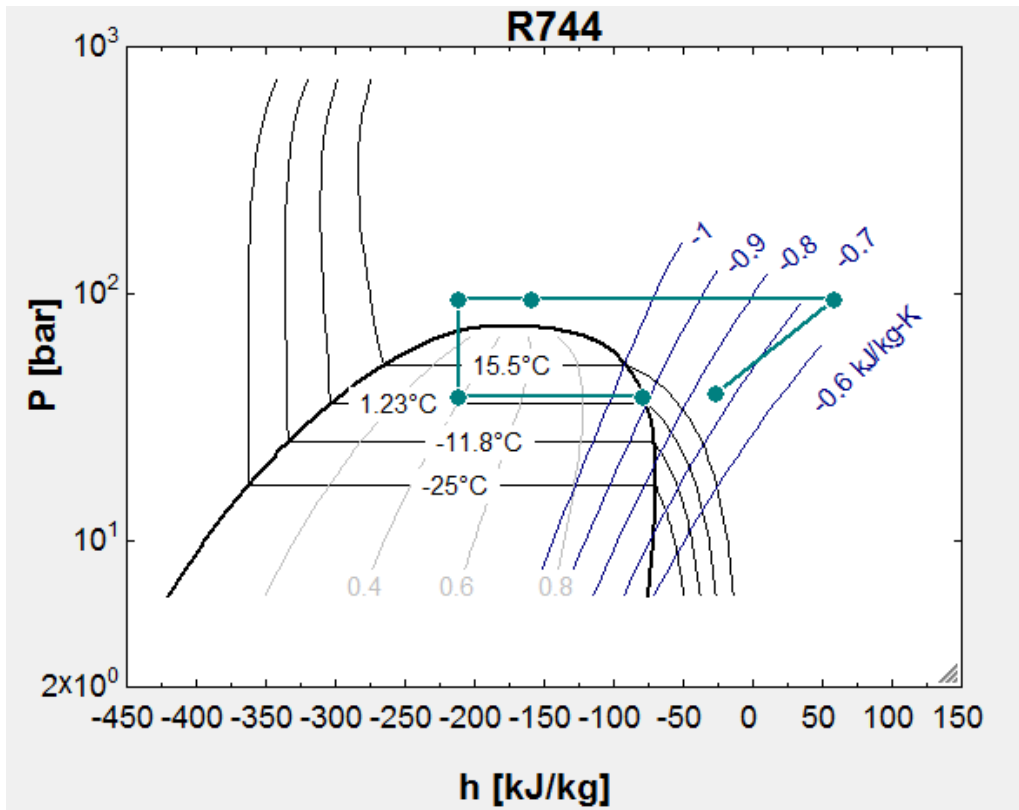
	1	2	3	4	5
	$T_i$ [C]	$P_i$ [bar]	$h_i$ [kJ/kg]	$s_i$ [kJ/kgK]	$x_i$
[1]	40	40	-26.68	-0.7447	100
[2]	142.9	95	58.8	-0.6448	100
[3]	42.72	95	-159	-1.269	-100
[4]	35.59	95	-210.8	-1.435	-100
[5]	4	38.69	-210.8	-1.394	0.3941
[6]	4	38.69	-78.53	-0.9167	1
[7]	30				
[8]	130.1				
[9]	30				
[10]	9.734				

**Table 7.** Table with properties values as output from TCHP with IHEX model

It is clear from the properties table (Table 7) and the following chart (Graph 6, Graph 7) that the quality out of the expansion valve ( $x_5$ ) is much smaller and so the graph has moved towards the center respecting the properties plot, in contrast to the relevant diagram that comes of the TCHP model without internal heat exchanger.

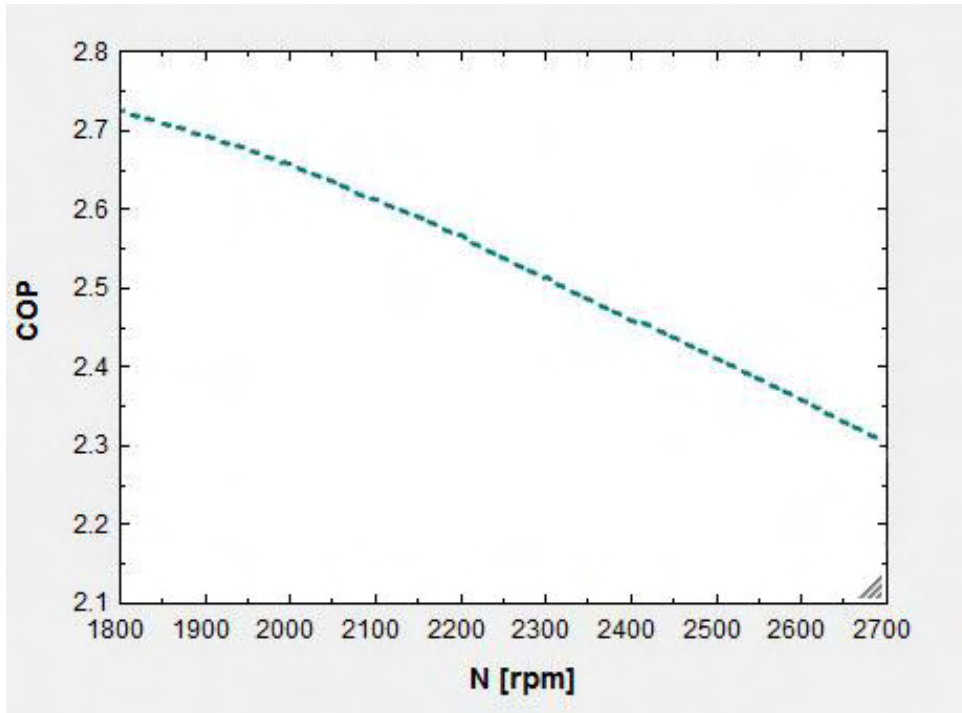


**Graph 6.** T-s diagram for TCHP with IHEX



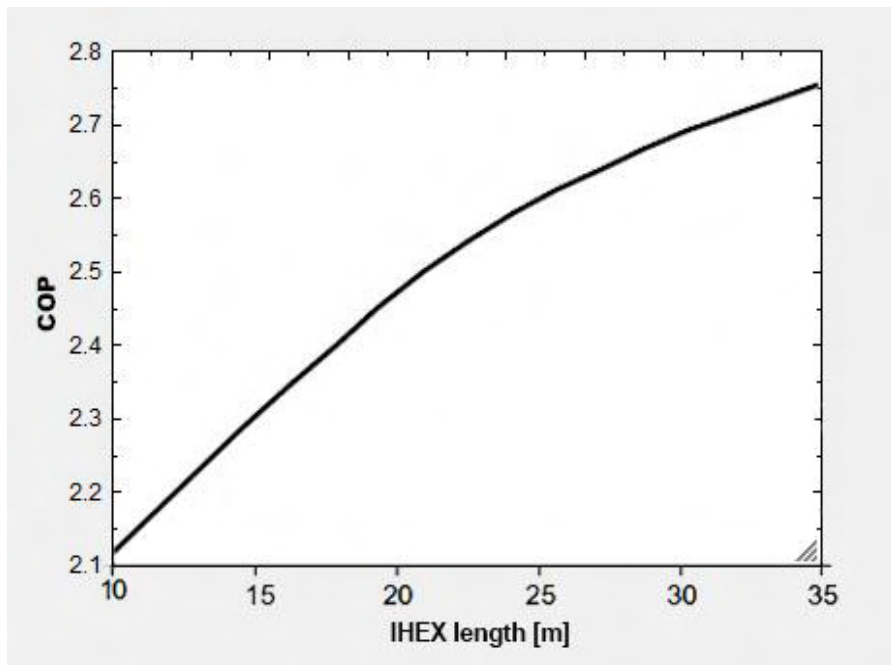
Graph 7. P-h diagram for TCHP with IHX

Another diagram that was derived is the variation of the coefficient of performance relatively to compressor speed. As we can see, the system COP is reduced as the compressor speed is increased. This is because the increasing speed leads to an increasing work of compressor and subsequently the COP is reducing.



**Graph 8.** COP variation over compressor speed for TCHP with IHEX

Furthermore, the Graph 9 shows the way that COP changes as the total length of internal heat exchanger, and consequently the effectiveness of the IHEX, increases.



**Graph 9.** COP variation respect to length of IHEX

#### 4.4. TCHP model with expansion recovery work with turbine

Besides the models that were developed, during this thesis, concerning the use or not of an internal heat exchanger, was studied the way of expansion. So a model that uses a turbine instead of an expansion valve was developed, in order to reduce losses through the valve and improve the exergetic efficiency with work recovery.

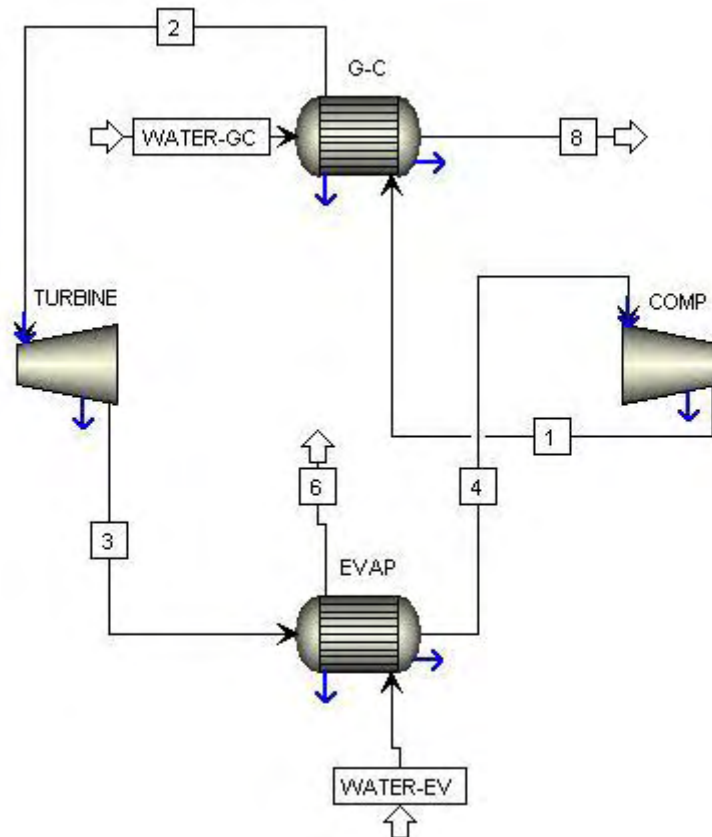


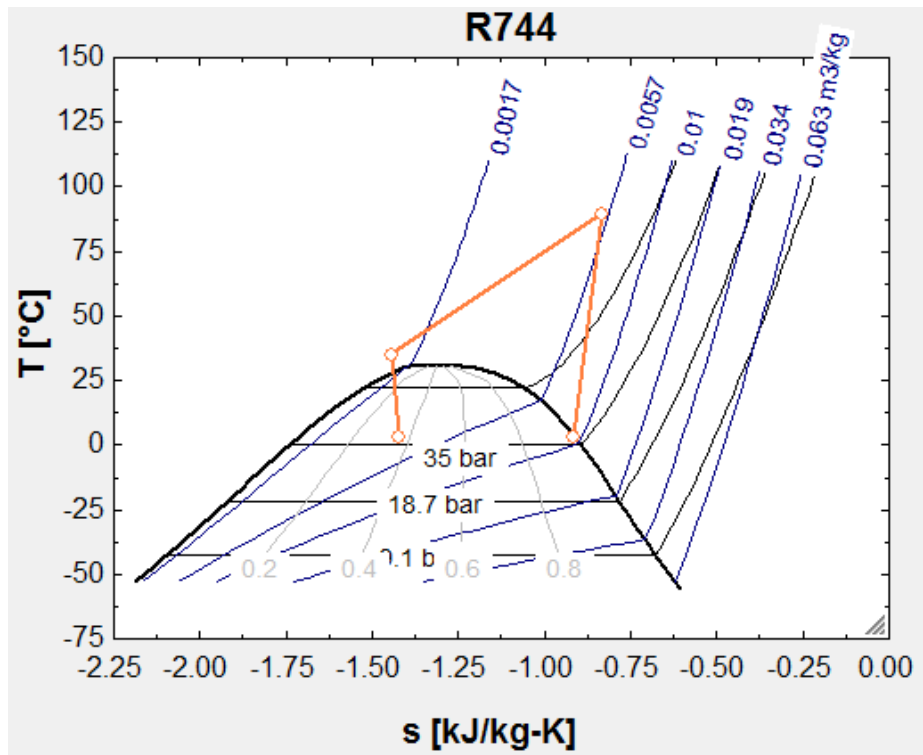
**Figure 31.** TCHP with an expansion turbine designed with ASPEN

The Table 8 contains the values of the properties derived from the TCHP with expansion recovery work using a turbine, so the stages are for compressor (1→2), gas-cooler (2→3), turbine (3→4) and evaporator (4→1). The situations 7, 8 and 9, 10 refer to the temperature of water at inlet and outlet of gas cooler and evaporator respectively.

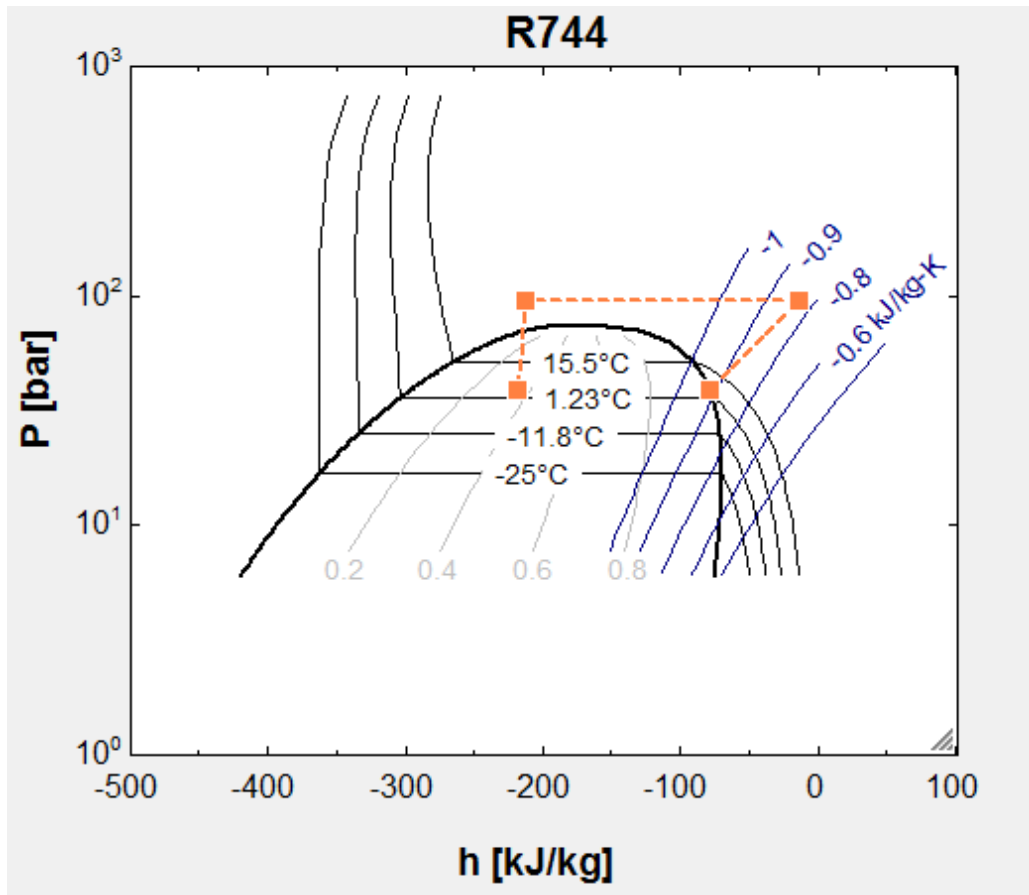
	1	2	3	4	5
	$T_i$	$P_i$ [kPa]	$h_i$ [kJ/kg]	$s_i$ [kJ/kg-K]	$x_i$
[1]	4	38.69	-78.53	-0.9167	1
[2]	90.08	95	-13.73	-0.8317	100
[3]	35.22	95	-212.5	-1.441	100
[4]	4	38.69	-219.3	-1.425	0.3552
[5]					
[6]	30				
[7]	78.56				
[8]	30				
[9]	22.24				

**Table 8.** Properties values as output from TCHP model with turbine

Observing the following temperature-entropy graph (Graph 10) and pressure-enthalpy graph (Graph 11), we can see that quality at the turbine outlet is even smaller than the model with IHEx and so the graph is moved more toward the center of the graph. As a consequence, the COP has increased and its maximum value surpasses 3, as the net work is smaller due to the use of an expansion turbine that reduces expansion irreversibilities.

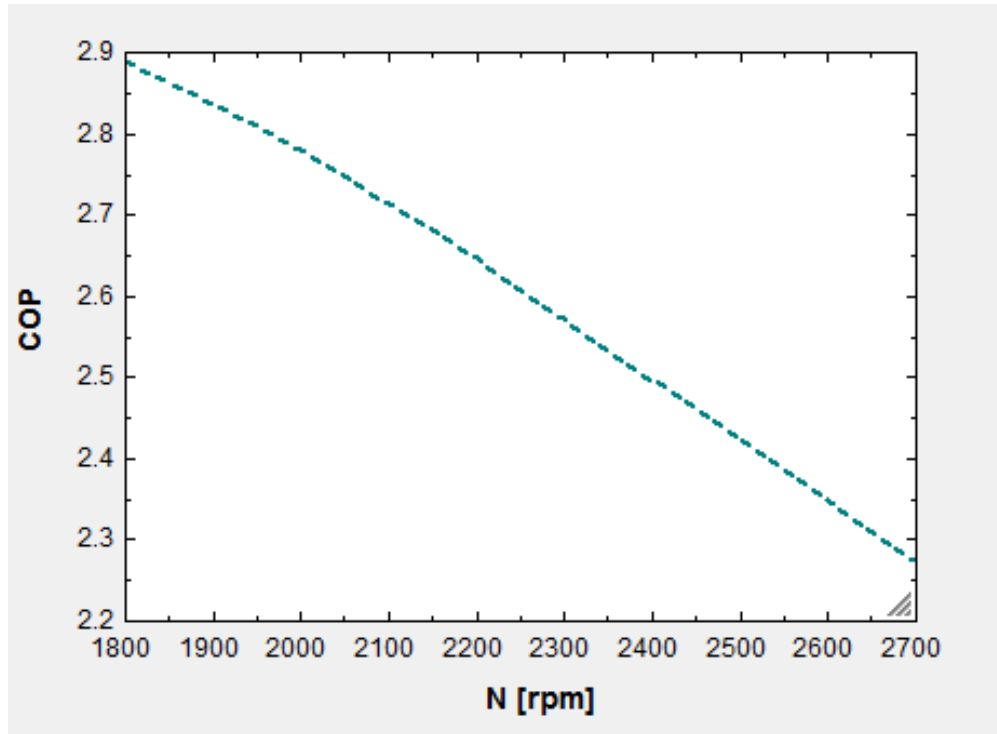


**Graph 10.** T-s diagram with TCHP model with an expansion turbine



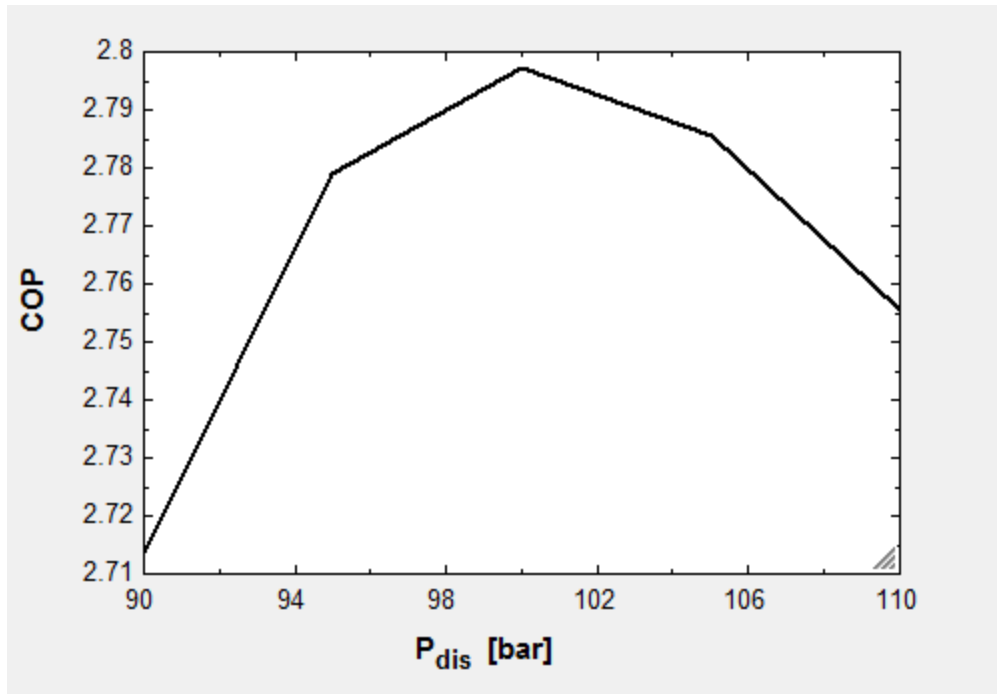
**Graph 11.** P-h diagram with TCHP model with an expansion turbine

Moreover, the performance of the system concerning the variation of COP respecting compressor's speed is the same with the previous models, with the difference of course that this model presents a better COP as maximum value.

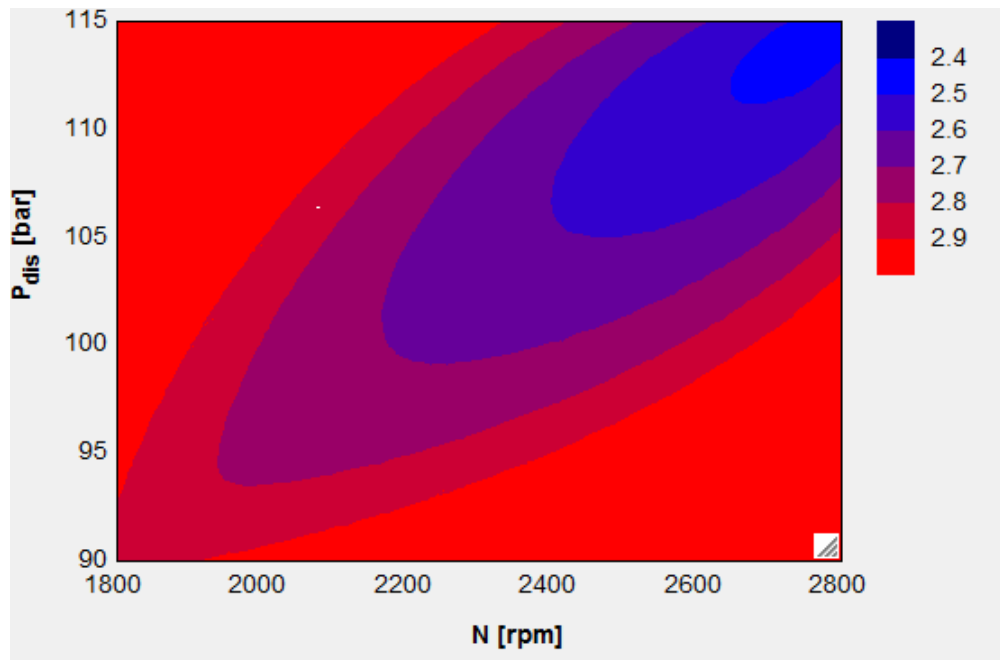


**Graph 12.** COP variation over compressor's rotational speed

Finally, we can see how the system's COP varies as a function of the discharge pressure and we can see that there is an increasing COP until 100 bar and then COP is reducing again (Graph 13). Also, at the Graph 14 we can see a contour diagram of COP as a function of discharge pressure and compressor's speed, where we can see that maximum COP is at smaller speed and a discharge pressure about 95 bar.



**Graph 13.** COP variation over discharge pressure for TCHP with an expansion turbine



**Graph 14.** Contour for COP as a function of discharge pressure and compressor's speed

## 5. Conclusions

Carbon dioxide was used as a refrigerant in some of the earliest refrigeration systems. CO<sub>2</sub> fell out of favor when other refrigerants delivered superior performance over a wider range of conditions. In light of growing concerns over climate change, CO<sub>2</sub> has been revived as a potential refrigerant due to its benign environmental qualities. To overcome limitations imposed by CO<sub>2</sub>'s low critical point, most of the research has focused on the use of CO<sub>2</sub> in a transcritical cycle. Due to the high working pressures and the distinct nature of the transcritical cycle, optimization of system components and process parameters is ongoing.

The models that were developed showed us that with the addition of an internal heat exchanger the COP can be increased about 5.5% (from 2.63 to 2.76). Also, we had a larger heating and cooling capacity after the use of an IHX.

Moreover, we have seen that there is an optimum discharge pressure that leads to an optimum COP and we have taken the corresponding graphs. Furthermore, with the use of a turbine instead of a throttling valve in order to expand the refrigerant, we improved the maximum COP from 2.76 to 2.92, which corresponds to an increase of 5.4% of the maximum system's COP with an expansion valve and an IHX. Also for the model with expansion recovery work through a turbine, we can see from the contour diagram for COP that the best combination is a low compressor speed and a discharge pressure about 95 bar.

## 6. Future work

All the modifications that can be studied and improve the performance of a TCHP, consist the subject of future research. The modifications that concern the compression, such as multi-stage compression, the expansion, such as the use of capillary tubes or an ejector instead of the throttling valve and some other schemes like flash-gas bypass model, will be examined and the models will be developed respectively and finally a comparative analysis over COP, discharge pressure and heating or cooling capacity will be completed. Furthermore, it is indispensable to investigate the transport characteristics for each case and the equations that govern each situation, issues under investigation because of the complicity of these phenomena.

Moreover, further analysis with more special software like ASPEN for the comparison of the results or by the construction of codes in one software language in order to make the convergence of the numerical schemes more manageable would be very profitable.

## Bibliography

- [1] B. T. Austin and K. Sumathy, "Transcritical CO<sub>2</sub> a review carbon dioxide heat pump systems: A review," *Renewable and Sustainable Energy Reviews* vol. 4013-4029, 2011.
- [2] P. Nekså, "CO<sub>2</sub> heat pump systems," *International Journal of Refrigeration*, vol. 25, pp. 421-427, 2002.
- [3] J. Stene, "INTEGRATED CO<sub>2</sub> HEAT PUMP SYSTEMS FOR SPACE HEATING AND HOT WATER HEATING IN LOW-ENERGY HOUSES AND PASSIVE HOUSES."
- [4] G. Lorentzen, "The use of natural refrigerants: a complete solution to the CFC/HCFC predicament," *International Journal of Refrigeration*, vol. 18, pp. 190-197, 1995.
- [5] J. L. Yang, Y. T. Ma, M. X. Li, and H. Q. Guan, "Exergy analysis of transcritical carbon dioxide refrigeration cycle with an expander," *Energy*, vol. 30, pp. 1162-1175, 2005.
- [6] J. Sarkar, "Review on cycle modifications of transcritical CO<sub>2</sub> refrigeration and heat pump systems," *Journal of Advanced Research in Mechanical Engineering*, vol. 1, pp. 22-29, 2010.
- [7] D. M. Robinson and E. A. Groll, "Efficiencies of transcritical CO<sub>2</sub> cycles with and without an expansion turbine: Rendement de cycles transcritiques au CO<sub>2</sub> avec et sans turbine d'expansion," *International Journal of Refrigeration*, vol. 21, pp. 577-589, 1998.
- [8] A. Cavallini, L. Cecchinato, M. Corradi, E. Fornasieri, and C. Zilio, "Two-stage transcritical carbon dioxide cycle optimisation: A theoretical and experimental analysis," *International Journal of Refrigeration*, vol. 28, pp. 1274-1283, 2005.
- [9] N. Agrawal and S. Bhattacharyya, "Studies on a two-stage transcritical carbon dioxide heat pump cycle with flash intercooling," *Applied Thermal Engineering*, vol. 27, pp. 299-305, 2007.
- [10] L. Cecchinato, M. Chiarello, M. Corradi, E. Fornasieri, S. Minetto, P. Stringari, *et al.*, "Thermodynamic analysis of different two-stage transcritical carbon dioxide cycles," *International Journal of Refrigeration*, vol. 32, pp. 1058-1067, 2009.
- [11] N. Agrawal and S. Bhattacharyya, "Adiabatic capillary tube flow of carbon dioxide in a transcritical heat pump cycle," *International Journal of Energy Research*, vol. 31, pp. 1016-1030, 2007.
- [12] J. Sarkar and N. Agrawal, "Performance optimization of transcritical CO<sub>2</sub> cycle with parallel compression economization," *International Journal of Thermal Sciences*, vol. 49, pp. 838-843, 2010.
- [13] J. Sarkar, S. Bhattacharyya, and M. R. Gopal, "Simulation of a transcritical CO<sub>2</sub> heat pump cycle for simultaneous cooling and heating applications," *International Journal of Refrigeration*, vol. 29, pp. 735-743, 2006.
- [14] J. Sarkar, S. Bhattacharyya, and M. Ram Gopal, "Natural refrigerant-based subcritical and transcritical cycles for high temperature heating," *International Journal of Refrigeration*, vol. 30, pp. 3-10, 2007.
- [15] J. Sarkar, S. Bhattacharyya, and M. Ram Gopal, "Transcritical CO<sub>2</sub> heat pump systems: exergy analysis including heat transfer and fluid flow effects," *Energy Conversion and Management*, vol. 46, pp. 2053-2067, 2005.

- [16] S. D. White, M. G. Yarrall, D. J. Cleland, and R. A. Hedley, "Modelling the performance of a transcritical CO<sub>2</sub> heat pump for high temperature heating," *International Journal of Refrigeration*, vol. 25, pp. 479-486, 2002.
- [17] J. L. Yang, Y. T. Ma, M. X. Li, and J. Hua, "Modeling and simulating the transcritical CO<sub>2</sub> heat pump system," *Energy*, vol. 35, pp. 4812-4818, 2010.
- [18] F. Zhang, P. Jiang, Y. Lin, and Y. Zhang, "Efficiencies of subcritical and transcritical CO<sub>2</sub> inverse cycles with and without an internal heat exchanger," *Applied Thermal Engineering*, vol. 31, pp. 432-438, 2011.
- [19] T. M. Ortiz, D. Li, and E. A. Groll, "Evaluation of the performance potential of CO<sub>2</sub> as a refrigerant in air-to-air air conditioners and heat pumps: system modeling and analysis," *Ray W. Herrick Labs Research Report HL 2003*, vol. 20, 2003.
- [20] S. H. Yoon, J. H. Kim, Y. W. Hwang, M. S. Kim, K. Min, and Y. Kim, "Heat transfer and pressure drop characteristics during the in-tube cooling process of carbon dioxide in the supercritical region," *International Journal of Refrigeration*, vol. 26, pp. 857-864, 2003.
- [21] V. Gnielinski, "New equations for heat and mass transfer in the turbulent flow in pipes and channels," *NASA STI/Recon Technical Report A*, vol. 75, p. 22028, 1975.
- [22] S. S. Pitla, E. A. Groll, and S. Ramadhyani, "New correlation to predict the heat transfer coefficient during in-tube cooling of turbulent supercritical CO<sub>2</sub>," *International Journal of Refrigeration*, vol. 25, pp. 887-895, 2002.
- [23] L. Cheng, G. Ribatski, and J. R. Thome, "Analysis of supercritical CO<sub>2</sub> cooling in macro- and micro-channels," *International Journal of Refrigeration*, vol. 31, pp. 1301-1316, 2008.
- [24] J. Sarkar, S. Bhattacharyya, and M. R. Gopal, "Optimization of a transcritical CO<sub>2</sub> heat pump cycle for simultaneous cooling and heating applications," *International Journal of Refrigeration*, vol. 27, pp. 830-838, 2004.
- [25] J. Sarkar, S. Bhattacharyya, and M. Ramgopal, "A transcritical CO<sub>2</sub> heat pump for simultaneous water cooling and heating: Test results and model validation," *International Journal of Energy Research*, vol. 33, pp. 100-109, 2009.
- [26] J. Sarkar, S. Bhattacharyya, and M. Ram Gopal, "Irreversibility minimization of heat exchangers for transcritical CO<sub>2</sub> systems," *International Journal of Thermal Sciences*, vol. 48, pp. 146-153, 2009.
- [27] S. H. Yoon, E. S. Cho, Y. W. Hwang, M. S. Kim, K. Min, and Y. Kim, "Characteristics of evaporative heat transfer and pressure drop of carbon dioxide and correlation development," *International Journal of Refrigeration*, vol. 27, pp. 111-119, 2004.